

# Extrapolative Weight Averaging Reveals Correctness-Efficiency Frontiers in Code RL

Kunhao Zheng<sup>1,2</sup>, Pierre Chambon<sup>1</sup>, Juliette Decugis<sup>1</sup>, Jonas Gehring<sup>1</sup>, Taco Cohen<sup>1</sup>, Benjamin Negrevergne<sup>2</sup>, Gabriel Synnaeve<sup>1</sup>

<sup>1</sup>Meta Superintelligence Labs - FAIR, <sup>2</sup>Université Paris-Dauphine PSL

Linear interpolation between fine-tuned checkpoints has been shown to trace the Pareto front between competing objectives, but whether *extrapolative weight averaging* can extend such frontiers to new checkpoints useful at inference time, without additional RL training, remains unclear. We study this question in RL for competitive programming, where hidden unit tests under time and memory limits enforce both functional correctness and computational efficiency. Starting from a shared initialization, we train checkpoints under nested unit-test coverage: low-coverage rewards require passing smaller-input tests, while high-coverage rewards require passing progressively larger tests up to the full suite. This sweep reveals the emergence of a *correctness-efficiency frontier*: on hard problems, higher-coverage reward reduces optimization failures but increases correctness failures, leaving solve rate nearly unchanged. Interpolation between low- and high-coverage checkpoints recovers this frontier, while extrapolation extends it beyond the trained endpoints. Both the frontier and its extrapolative continuation appear across three inference settings, pure reasoning, tool use, and agentic coding, and across two model scales, 32B and 7B. At the problem level, moving along the frontier changes which problems are solved, making extrapolated checkpoints complementary policies in inference-time scaling. Ensembles with extrapolative weight averaging broaden coverage and improve pass@250 on LCB/hard by 3.3% over the best single checkpoint at matched sample budget. These results show that nested unit-test coverage in code RL induces a frontier that extrapolative weight averaging can navigate, extend, and exploit.

Date: May 28, 2026

Correspondence: Kunhao Zheng at [kunhao@meta.com](mailto:kunhao@meta.com)

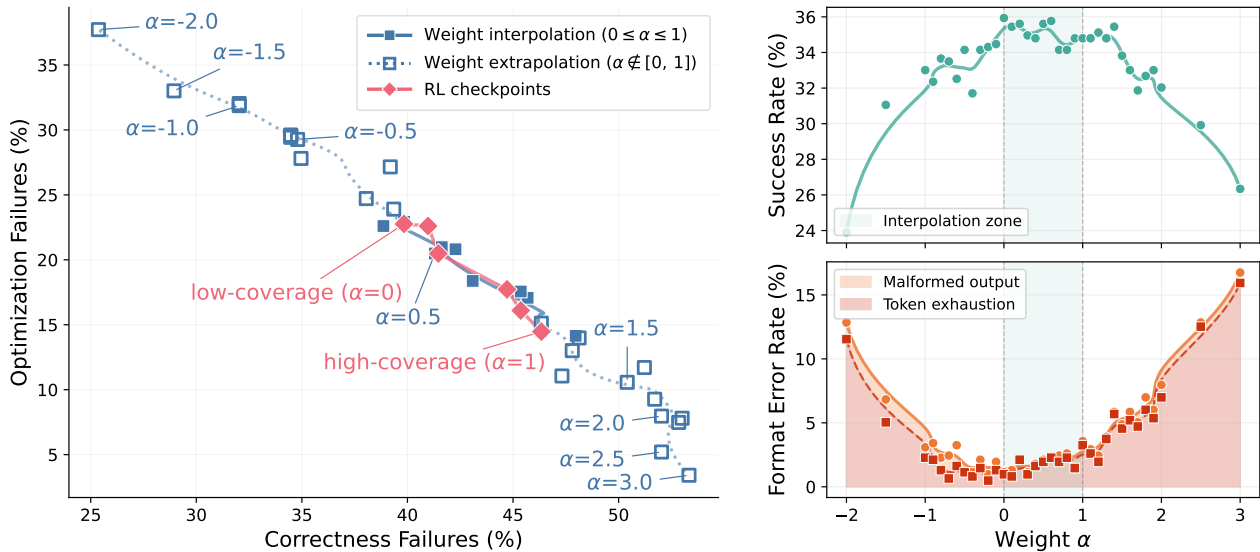


**Figure 1** Linear interpolation and extrapolation between two RL checkpoints (trained under tool-use setting) on LCB/hard. **Left:** extrapolated checkpoints continue the same correctness-efficiency frontier traced by interpolated and independently trained RL checkpoints beyond any single RL training run produces. **Right:** solve rate is stable across the interpolation interval and a wide extrapolation regime, and degrades only at extreme  $|\alpha|$  where format errors rise sharply through token exhaustion.

# 1 Introduction

Weight averaging offers a simple way to navigate between related checkpoints. Prior work shows that checkpoints sharing an initialization can often be averaged without destroying performance, and that interpolation in RL can trace trade-offs between training objectives (Frankle et al., 2020; Wortsman et al., 2022; Ilharco et al., 2023; Ramé et al., 2023). Most of this work stays inside the convex hull of trained checkpoints. The question we ask is whether extrapolation between related RL checkpoints can continue a learned frontier beyond that hull, without additional training. To answer this cleanly, we need a checkpoint family that shares an initialization, varies along an ordered axis, and differs in a semantically interpretable way.

Competitive programming provides exactly this kind of setting since a solution is expected to be both correct and algorithmically efficient. Relaxed tests can reward brute-force programs that work on small inputs, whereas larger stress tests reject the same programs under the problem’s time and memory limits. This makes verifier strictness a natural experimental axis for code RL. We vary strictness through nested input-size thresholds, so stricter rewards demand success on progressively larger tests while keeping the task distribution and initialization fixed. Starting from a shared SFT checkpoint, we train independent RL runs under several coverage levels to control the reward strictness, producing an ordered family of checkpoints along a single interpretable axis.

On hard problems, this ordered family does not collapse to a simple ranking by reward strictness. Instead, it traces a *correctness-efficiency frontier*. This frontier gives extrapolative weight averaging a concrete target: interpolation should recover the known verifier-induced axis, while extrapolation tests whether the same axis continues beyond the checkpoints produced by RL (Figure 1).

We organize the paper around three questions:

1. **What frontier does nested unit-test coverage create?** Nested coverage gives a controlled axis along which stricter rewards reduce optimization failures but increase correctness failures on capability-matched problems, leaving solve rate nearly unchanged (Section 3.1).
2. **Can extrapolative weight averaging go beyond trained checkpoints?** Interpolation between low- and high-coverage endpoints recovers the frontier traced by independently trained checkpoints, while extrapolation continues the same frontier beyond the RL endpoints. This continuation appears across pure reasoning, tool use, agentic coding, and the model scales we study (Sections 3.2-3.4).
3. **Why is extrapolative weight averaging useful?** Extrapolated checkpoints are complementary policies: they solve different hard problems. Ensembling checkpoints along the extended frontier converts this complementarity into broader solved-set coverage, improving LCB/hard pass@250 by 3.3% over the best single checkpoint under matched sample budget, with more diversity. (Section 4.1).

Section 4.2 delimits the claim: static reward shaping over the same nested outcomes stays on the frontier, while failure-conditioned training provides an exploratory contrast for what additional information may move the frontier itself.

## 2 Extrapolative Weight Averaging: Hypothesis and Setup

We study linear weight averaging between two RL checkpoints  $\theta_A$  and  $\theta_B$ ,

$$\theta_\alpha = \alpha \theta_B + (1 - \alpha) \theta_A, \tag{1}$$

where  $\alpha \in [0, 1]$  gives interpolation and  $\alpha \notin [0, 1]$  gives extrapolation. The first empirical check is interpolation: if this arithmetic is meaningful in our setting, interpolated checkpoints should recover sensible behavior between the trained endpoints, in line with prior results (Ramé et al., 2023). The main question is whether the same arithmetic remains meaningful outside the interval spanned by trained checkpoints.

This question is meaningful only when  $\alpha$  corresponds to one controlled difference: they should share an initialization, differ along a single interpretable axis, and keep the rest of training fixed. Otherwise the averaging direction mixes several changes at once, and behavior outside the trained interval is hard to attribute to one underlying cause.

Verifier strictness in competitive programming provides such an axis. Relaxed tests reward programs that pass smaller inputs, whereas stricter tests increasingly demand asymptotically efficient algorithms. This leads to a concrete hypothesis: RL checkpoints trained under progressively stricter rewards may induce a correctness-efficiency frontier. If they do, interpolation should recover that frontier and extrapolation may continue it beyond the checkpoints that RL itself produced. We instantiate this axis as follows.

**Training family.** We instantiate the verifier-strictness sweep separately in three RL settings of increasing interaction capability: **pure reasoning**, which generates code after single-turn reasoning; **tool use**, which interleaves reasoning and Python tool call in multi turns; and **agentic coding**, which uses a sandboxed terminal with file-system access. In each setting, we train independent RL runs from a shared SFT checkpoint on CodeContestsPlus (Wang et al., 2025) ( $1\times$  variant), under a nested family of unit-test rewards indexed by the input-length threshold  $10^k$ :

$$R_k(y) = \mathbf{1}[y \text{ passes every test with input length } < 10^k], \quad R_\infty(y) = \mathbf{1}[y \text{ passes every test}]. \quad (2)$$

Lower  $k$  accepts more submissions; higher  $k$  demands asymptotically efficient algorithms. We sweep  $k \in \{2, \dots, 6, \infty\}$  to span the no-pressure to strict-pressure endpoints, with this range chosen by the unit test distributions in CodeContestsPlus (Appendix C.1).

**Evaluation.** We evaluate checkpoints sampled throughout training, including the final checkpoints, on the same held-out benchmark with full test coverage. The benchmark is LiveCodeBench (LCB) v5 (Jain et al., 2025) (20240801-20250201), with easy, medium, and hard split.

**Outcome taxonomy.** We sort each problem’s tests by input size and stop at the first failing test, which classifies every code submission into one of four mutually exclusive outcomes: **correct** (all tests pass), **optimization failure** (resource limit exceeded after passing all smaller ones), **correctness failure** (wrong answer or runtime exception within resource limits), and **format error** (unparsable output). Optimization failure does not guarantee algorithmic correctness; a submission may contain a bug masked by the resource limit. To validate our design, Appendix I shows that the main trade-off is robust to timeout-label ambiguity under extended time budgets and LLM-based judgment, and Appendix I.2 shows that memory exhaustion is a non-trivial part of optimization failure.

**Models.** We study at both 32B and 7B scale, in both cases we start from a pre-RL SFT checkpoint to ensure that we study the effect of RL itself rather than layering RL on an already RL-trained model. We run extended RL for thousands of steps, to check whether the observation continues to hold over longer training. For 32B model, we use CWM-SFT (FAIR CodeGen team et al., 2025). Specially for tool-use environment, we conduct two iterations of rejection sampling to teach the tool-call format and use the resulting checkpoint as the starting policy of our experiments (Appendix C.5). For 7B model, since Qwen-2.5 7B (Qwen et al., 2025) does not provide a public pre-RL SFT reasoning checkpoint, we fine-tune its base model ourselves on the public OpenCodeReasoning-2 (Ahmad et al., 2025) and OpenMathReasoning (Moshkov et al., 2025), giving us full control and transparency over the SFT datamix. Training details are in Appendices C.2 and C.5.

### 3 Extrapolation Extends the Correctness-Efficiency Frontier

We first establish the prerequisite empirical structure for the paper: varying verifier strictness induces a frontier between optimization failures and correctness failures on hard problems (Section 3.1). We then test the hypothesis: linear interpolation recovers this frontier (Section 3.2), and linear extrapolation continues it beyond what any single RL run reaches (Section 3.3). We close by showing a strong generalization of both the frontier and its extension by extrapolative weight averaging across RL environment settings and model scales (Section 3.4).

#### 3.1 A Correctness-Efficiency Frontier from Verifier-Strictness Sweeps

On held-out LCB/hard problems, stricter verifier coverage does not steadily raise solve rate. Instead, it organizes independently trained RL checkpoints into a narrow frontier: relaxed coverage produces more

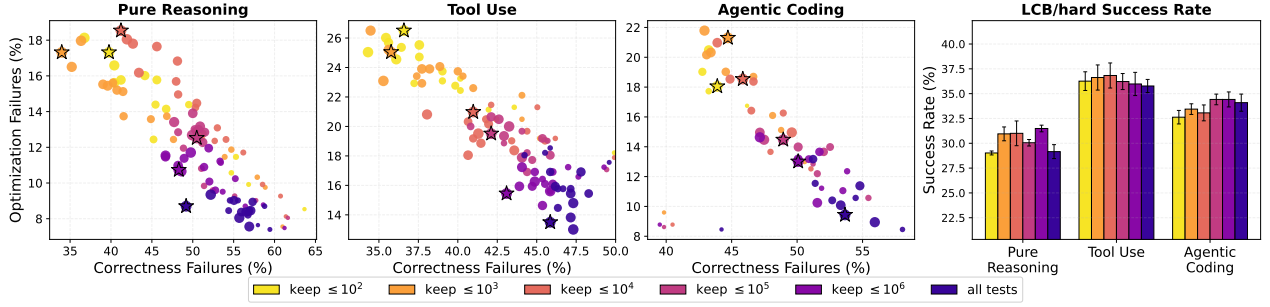


**Figure 2** Correctness-efficiency frontier on LCB/hard across three inference settings. Each scatter panel shows checkpoints sampled throughout RL training under different coverage thresholds. Smaller points are earlier checkpoints, larger points are later checkpoints, and stars mark final checkpoints. In every setting, the training trajectories follow the same trade-off between optimization and correctness failures, defining the frontier we extrapolate along. **Right:** bars averaging the last four checkpoints at each threshold confirm that solve rate remains nearly unchanged across conditions in late training.

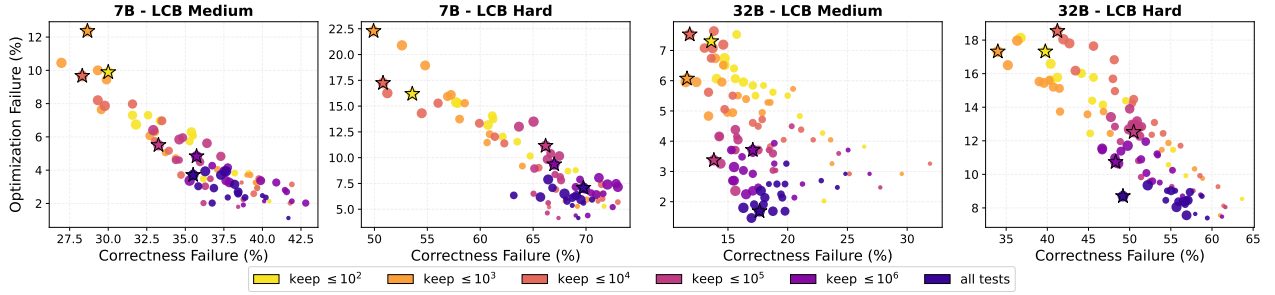


**Figure 3** Pure-reasoning evaluation at 7B and 32B on medium and hard splits. The trade-off appears only on hard problems at 32B, but already on medium problems at 7B, showing that the frontier tracks model capability rather than a fixed difficulty label.

optimization failures, stricter coverage produces more correctness failures, and late-training solve rates remain close across thresholds. Figure 2 shows this pattern throughout training across pure reasoning, tool use, and agentic coding.

Rather than attaching to one fixed benchmark label, the frontier appears wherever problems approach the model’s capability limit. Figure 3 shows this shift across scales: at 32B the frontier is clear on the hard split, whereas at 7B the same structure already appears on the medium split. In both cases, the frontier emerges once problem difficulty is high enough that correctness and efficiency genuinely compete. Taken together, these results give the rest of the section its starting geometry: verifier strictness creates an ordered family of checkpoints along a single behavioral axis. The next two subsections show that weight averaging can follow that axis directly, first by recovering the frontier through interpolation and then by extending it beyond the checkpoints reached by RL.

### 3.2 Linear interpolation recovers the frontier

Interpolation between a lower-coverage endpoint  $\theta_{\text{low}}$  and a higher-coverage endpoint  $\theta_{\text{high}}$ , namely  $\theta_\alpha = (1 - \alpha)\theta_{\text{low}} + \alpha\theta_{\text{high}}$  with  $\alpha \in [0, 1]$ , recovers the frontier traced by the independently trained verifier sweep. As  $\alpha$  moves from 0 to 1, solve rate stays nearly flat while optimization failures give way to correctness failures in a smooth progression (Figure 1). Two checkpoints therefore reconstruct the same trade-off that otherwise required a full family of RL runs. A single interpolation direction in weight space is sufficient to traverse that frontier.

Prior work shows that interpolation can navigate a multi-objective trade-off between checkpoints trained under different rewards (Ramé et al., 2023). In our case, the trade-off is not designed by specifying separate objectives since the rewards are nested and monotone improvement is plausible in theory. Empirically, the

verifier-strictness sweep traces out a frontier across separate RL runs, and interpolation recovers that same frontier.

### 3.3 Linear extrapolation extends the frontier beyond what RL reaches

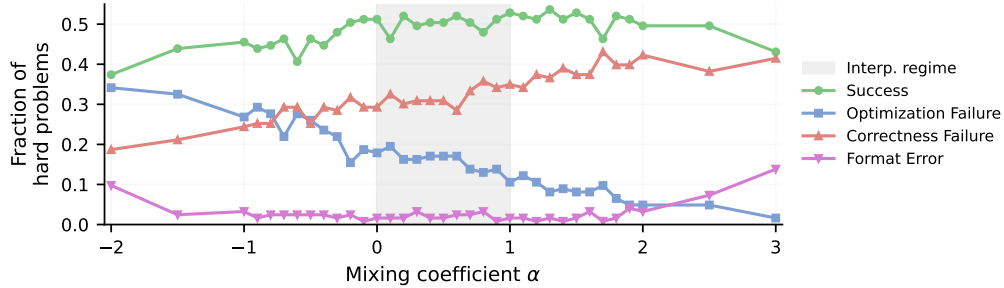


**Figure 4** Outcome composition along the interpolation and extrapolation axis on LCB/hard for RL checkpoints (trained under tool-use setting). The interpolation coefficient  $\alpha$  moves from the lower-coverage endpoint  $\theta_{low}$  at  $\alpha = 0$  to the higher-coverage endpoint  $\theta_{high}$  at  $\alpha = 1$ . Optimization failures fall as correctness failures rise, while solve rate remains nearly flat across the interpolation regime and a broad extrapolation range. Format errors become substantial only at extreme  $|\alpha|$ . The grey band marks the interpolation interval  $[0, 1]$ .

Extrapolation continues the same frontier beyond the checkpoints reached by RL (Figure 1). For  $\alpha > 1$ , the extrapolated checkpoints move past the higher-coverage endpoint towards fewer optimization failures and more correctness failures than RL itself reaches. For  $\alpha < 0$ , they continue the same trade-off in the opposite direction beyond the lower-coverage endpoint. Extrapolative weight averaging therefore does more than recover the verifier-strictness sweep. It extends that sweep to new checkpoints that no single RL run produces.

This continuation remains stable over a broad range of extrapolation coefficients. For  $\alpha \in [-0.5, 1.5]$ , solve rate stays nearly flat even though this interval already extends beyond the two trained endpoints, while optimization failures fall and correctness failures rise along the same pattern seen inside the trained interval (Figure 4). At more extreme coefficients, the same pattern remains visible, but solve rate drops because format errors rise sharply, mostly through token exhaustion. Extrapolative weight averaging therefore extends the verifier-strictness sweep beyond the range reached by RL, until model generations collapse.

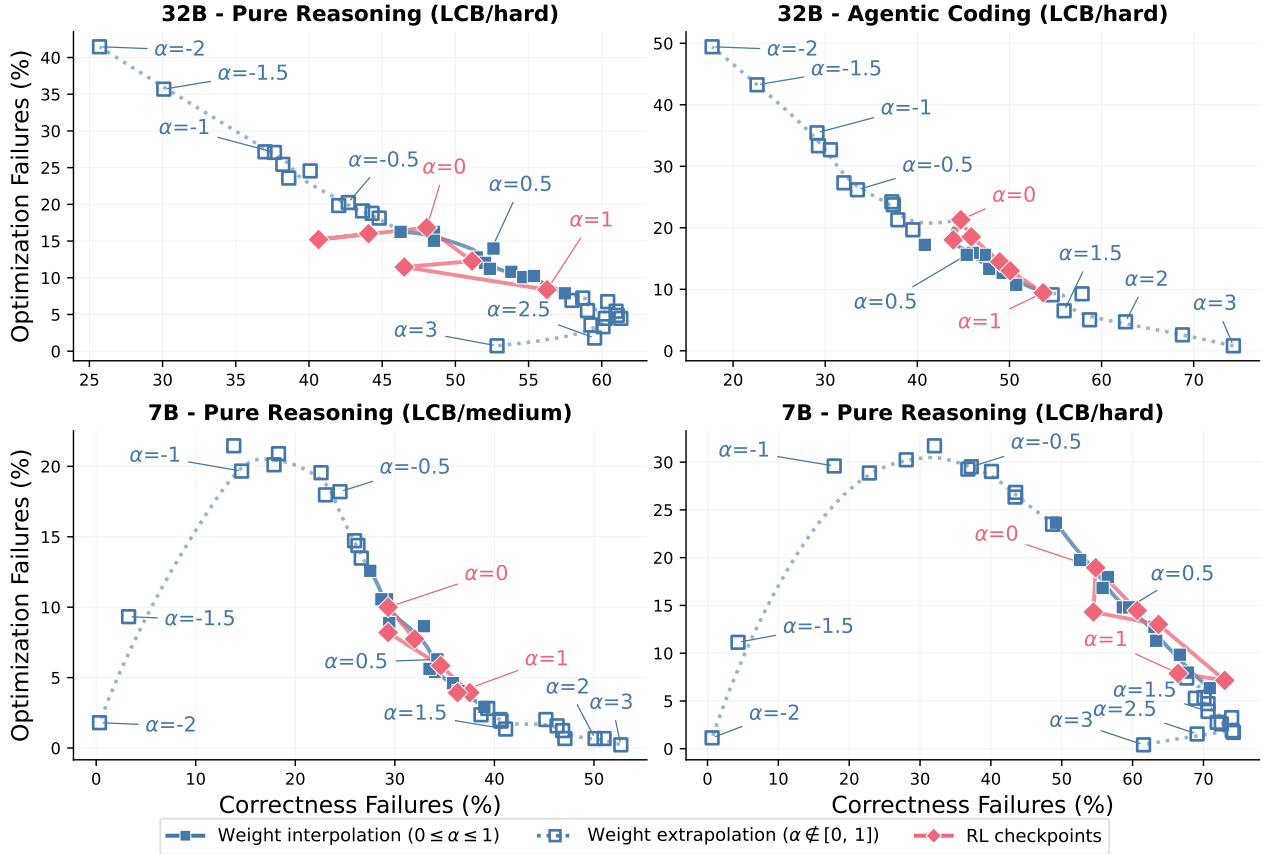
### 3.4 Extrapolative weight averaging generalizes across inference settings and model scales

Figure 5 extends the 32B tool-use case in Figure 1 to the two remaining 32B inference settings. In both pure-reasoning and agentic coding, interpolation recovers the correctness-efficiency frontier inside the trained interval, and extrapolation continues the same frontier beyond it. Agentic coding shows the cleanest continuation. Pure reasoning follows the same trend, but with visibly more scatter and earlier degradation at extreme coefficients.

The scale comparison follows the same capability-relative pattern as Section 3.1. For the 7B model, Figure 5 shows both LCB/medium and LCB/hard, which shows the same frontier and extrapolative continuation. The stable range for extrapolation is narrower at 7B, especially on the low- $\alpha$  side where format errors dominate once  $\alpha < -1$  (Appendix D.1). Extrapolative weight averaging therefore generalizes across inference settings and across model scale once problem difficulty is matched to model capability, while the width of the stable regime is setting dependent.

## 4 Analysis and Perspectives

Section 3 showed that extrapolative weight averaging extends the correctness-efficiency frontier beyond the RL endpoints. This section asks how that extended range can be used at inference time, and what it takes to move the frontier itself. Section 4.1 shows that moving along the axis changes which hard problems are solved, which makes ensembling extrapolated checkpoints useful for inference-time scaling. Section 4.2 offers



**Figure 5** Extrapolative continuation across inference settings and model scale. Figure 1 provides the 32B tool-use case. We show the two remaining 32B settings on LCB/hard, pure reasoning and agentic coding, and 7B pure reasoning on LCB/medium and LCB/hard. In each plot, interpolation recovers the correctness-efficiency frontier inside the trained interval, and extrapolation continues the same trade-off outside it, while the stable extrapolation range is narrower for 7B.

an exploratory contrast: static reward reshaping leaves the frontier intact, whereas richer failure information may begin to shift it.

#### 4.1 Per-problem turnover and inference-time ensembles

The nearly flat solve rate along the extrapolation axis conceals substantial per-problem turnover. On LCB/hard, 24.4% of problems are solved at every  $\alpha$ , 28.5% are never solved, and the remaining 47.2% are solved only on part of the axis (Figure 7). This middle band is the source of the solved-set diversity that ensembles can exploit. The frontier itself is broader: as  $\alpha$  varies, optimization failures and correctness failures also trade off among problems that remain unsolved throughout the sweep. Figure 6 shows that the solve-set turnover is gradual: adjacent values of  $\alpha$  share more than 80% of solved problems, and the overlap falls steadily to about 55% at the extremes.

This turnover gives the frontier axis a direct use at inference time. Instead of spending the full sampling budget on a single checkpoint, we can spread that budget across checkpoints along the axis and aggregate their candidates. Appendix E.2

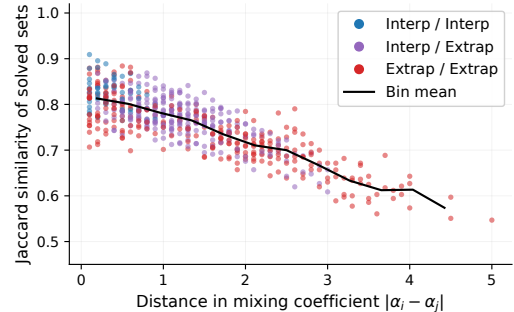


**Figure 6** Jaccard similarity of solved sets as a function of  $|\alpha_i - \alpha_j|$ . Overlap falls steadily with distance in  $\alpha$  for interpolation, extrapolation, and mixed pairs.



**Figure 7** Per-problem outcomes across weight-averaging coefficients  $\alpha$ , sorted into always-solved (top), partially solved (middle), and never-solved (bottom). The middle group (47.2%) accounts for the changes in which problems are solved. Failure types also continue to trade off among never-solved problems throughout the sweep.

shows the coverage headroom: the union over interpolated checkpoints reaches 79 of 123 hard problems, and admitting extrapolated checkpoints raises this to 88.

Figure 8 compares three matched-budget designs on LCB/hard: sampling from the best single checkpoint, splitting the budget across five interpolated checkpoints with  $\alpha \in [0, 1]$ , and splitting it across five checkpoints selected from the larger interpolation-plus-extrapolation range. Each method uses the same total sampling budget per problem. The interpolation-only pool helps modestly at larger candidate budgets. The pool that includes extrapolated checkpoints improves pass@250 by 3.3% over the best single checkpoint (problem-level bootstrap 95% CI: [0.8%, 6.5%]), suggesting that extrapolated checkpoints add complementary solutions beyond what interpolation alone provides.

Without filtering, the extrapolation-inclusive pool can be weaker than the best single checkpoint at small submission budgets. The extra diversity from extrapolation also brings more correctness-failure noise, so when only a few submissions are allowed the correct solutions are easier to miss. We therefore evaluate public-test filtering, which is standard in the literature (Li et al., 2022; Gehring et al., 2025; Zheng et al., 2025b), and report pass  $n@k$ , which measures success rate when filtering from  $k$  candidates and allowing up to  $n$  submissions. Appendix E.3 gives the in-domain operating curve on LCB/v5: fixing  $k = 250$ , the extrapolation-aware pool is higher than both the best single checkpoint and the interpolation-only pool at each displayed submission budget  $n$ . Thus public-test filtering can carry part of the large-candidate-budget diversity gain to smaller submission budgets.

A natural concern is that checkpoint-pool selection may be tuned to LCB/v5. Figure 9 addresses this more directly: for each candidate budget  $k$ , we search for the best five-checkpoint pool on LCB/v5 and evaluate it on the newer LCB/v6 (20250201-20250501) hard split. The transferred pool becomes beneficial once both  $k$  and  $n$  are large enough. A pool selected directly on LCB/v6 still performs better, so extrapolation provides transferable diversity while better pool selection leads to potentially better performance.

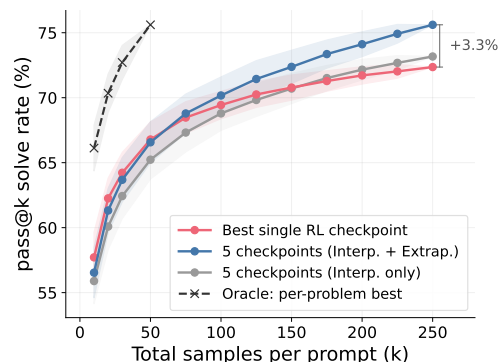


**Figure 8** Matched-budget pass@ $k$  on LCB/hard. The best ensemble using both interpolation and extrapolation outperforms the best single checkpoint and the best interpolation-only ensemble.

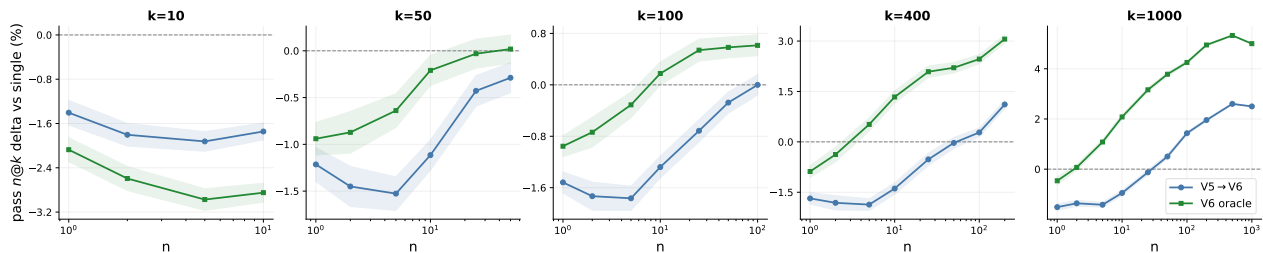


**Figure 9** Transfer of checkpoint-pool selection from LCB/v5 to LCB/v6 on the hard split. For each candidate budget  $k$ , we first select the best five-checkpoint pool on LCB/v5, then freeze that pool and evaluate the same checkpoints on LCB/v6. The blue curve is this transferred pool; the green curve is an oracle pool selected directly on LCB/v6. The y-axis reports the change in pass  $n@k$  relative to the best single checkpoint selected on LCB/v6. The transferred pool becomes beneficial at larger  $k$  and  $n$ , while the gap to the oracle shows that improvement leaves room for better pool selection methods.

## 4.2 What moves the frontier, and what does not

**The reward-shaped variants we tested stay on the frontier.** The discrete and continuous reward-shaped variants we tested both lie on the same LCB/hard frontier as the verifier-threshold runs. A simplified KL-regularized view helps explain why this is plausible: static reward shaping averages the same nested threshold rewards, so the shaped optimal policy remains tied to the same family of single-threshold optimal policies (Appendix F).

**Failure-conditioned training begins to shift the frontier.** We next ask whether failed attempts themselves provide training signal beyond a static reweighting of the same outcomes. In *online-fixing*, each failed rollout triggers additional worker-side sampling from a prompt built from the original problem, the failed code, and aggregated execution statistics. To separate information from budget, we keep trainer compute fixed, allow extra worker compute only adaptively after failures, and compare against a compute-matched *resample-only* control that uses the same extra adaptive worker compute but uses the original problem statement only. We evaluate both the original code-generation task, measured by pass@1 from the problem statement alone, and the repair task, measured by fix@1 given the failure context. The clearest case is 32B pure reasoning: relative to the matched control, online-fixing raises fix@1 on LCB/hard from 14.2% to 17.9% and pass@1 on full LCB from 61.2% to 62.6% (Appendix G.3). Outside this setting, transfer back to the original code-generation task is smaller and less consistent. We therefore treat this as exploratory evidence that richer failure information can begin to push the frontier outward at fixed trainer compute.

## 5 Related Work

**RL for code reasoning and test quality.** Reinforcement learning with verifiable rewards has become a standard post-training recipe for code reasoning, from single-turn generation to tool-integrated and agentic settings (Guo et al., 2025; Liu et al., 2025; MiniMax et al., 2025; Xue et al., 2025; FAIR CodeGen team et al., 2025; Kimi Team et al., 2026). Benchmarks such as CodeContests (Li et al., 2022), APPS (Hendrycks et al., 2021), and TACO (Li et al., 2023) established code generation under executable tests as a central evaluation setting. Later work sharpened the role of test quality, including EvalPlus (Liu et al., 2023), LiveCodeBench (Jain et al., 2025), and CodeContestsPlus (Wang et al., 2025). At inference time, a parallel line studies how additional inference compute improves code generation through larger candidate pools, public-test filtering, and iterative candidate refinement (Li et al., 2022; Zheng et al., 2025b; Li et al., 2025a). Other methods use simulated execution for self-fixing (Maimon et al., 2026) or trajectory reuse in agentic coding (Kim et al., 2026). During training, other work moves beyond a single outcome reward by adding richer execution-level or process-level signals, through execution feedback (Gehring et al., 2025), process-level rewards (Li et al., 2025b; Dai et al., 2025), and self-verification with generated tests (Jin et al., 2025).

**Linear mode connectivity, model merging and extrapolation.** Frankle et al. (2020) shows that vision networks trained from the same initialization can often be connected by low-loss linear paths. Model merging

exploits this structure through model souping (Wortsman et al., 2022), task vector editing (Ilharco et al., 2023), and layer-wise variants (Yang et al., 2024; Wang et al., 2024; Lin et al., 2024). Closest to our interpolation result is Rewarded Soups (Ramé et al., 2023), which shows that interpolating checkpoints trained under explicitly different rewards traces a multi-objective Pareto front. Follow-up work extends this idea to reward models and policy models (Ramé et al., 2024; Ramé et al., 2024). Our setting differs in that the checkpoints are trained under a nested family of stricter and looser verification regimes within the same binary pass-fail signal, rather than under explicitly different reward objectives. Recently, Neural Thickets (Gan and Isola, 2026) provides a complementary view of weight-space diversity through random perturbation and ensembling. For extrapolation, the nearest precedents are ExPO (Zheng et al., 2025a), AlphaRL (Cai et al., 2026) and Wang et al. (2026), which extrapolate along a single post-training trajectory (SFT-to-DPO or early-to-late RL). In our setting, by contrast, the extrapolation is *between two RL checkpoints*, and it continues the same frontier beyond what either training run reaches.

**Correctness and efficiency in code.** Recent work increasingly treats efficiency as an essential dimension of code quality alongside correctness. Mercury (Du et al., 2024) introduces efficiency-stratified evaluation to distinguish correct-but-slow solutions from efficient ones. ECCO (Waghjale et al., 2024) studies the tension between improving efficiency and preserving correctness in model-generated code. Related benchmarks extend this concern to algorithmic efficiency (Huang et al., 2024; Chambon et al., 2025), GPU kernels, and software engineering workloads (Ouyang et al., 2025; Ma et al., 2025). Afterburner (Du et al., 2025) uses a self-improving loop with RL to improve code efficiency. These works study settings where efficiency is made explicit, either in the benchmark or in the objective, leaving open what standard unit-test RL does when correctness and efficiency are folded into the same pass-fail supervision.

## 6 Discussion and Limitations

**Nested rewards need not yield nested policies.** In our setting, the rewards are nested by construction. However, empirically, the learned policies during on-policy RL are not ordered by dominance. Stricter verification does not produce a nested sequence of better checkpoints on hard problems. Instead, it moves policies along the frontier, trading off optimization failures and correctness failures. More broadly, nested rewards do not guarantee nested learned behavior, likely because on-policy RL changes which solution modes are reinforced.

**Extrapolative weight averaging turns sharpening into diversity.** The frontier is useful as its points are complementary policies, rather than one point dominates the others. Extrapolative weight averaging makes this complementary nature accessible beyond the checkpoints reached by individual RL runs. This gives a different view of RL sharpening effect (Yue et al., 2025; Cui et al., 2025; Wu et al., 2026): even if each checkpoint sharpens towards a particular solution mode, extrapolative weight averaging provides a controlled axis to vary which mode is favored. This points to two promising research directions. At inference time, how to design frontier-aware inference procedure to recover diversity by sampling across these sharpened policies. During RL training, how to incorporate weight extrapolation in the worker side to offer a way to increase rollout diversity.

**Beyond a single verifier frontier.** As preliminary evidence, Appendix A averages two checkpoints optimized for different sampling behavior: one with stronger pass@1 and one with stronger pass@ $k$ . Interpolation traces a smooth Precision-Recall curve, and yields ensembles that outperform single-checkpoint sampling at larger budgets. Although extrapolation adds only modest gains, the broader message is encouraging: extrapolative weight averaging may provide a cheap way to extend the frontier and navigate different behavior pattern, whenever a shared-initialization checkpoint pair lies on a meaningful frontier.

**Limitations.** Our experiments are confined to competitive programming domain, but they are not confined to a single RL environment setting. Our experiments show that the frontier appears across pure-reasoning, tool-use, and agentic coding, which span from single-turn generation to richer sandbox feedback, suggesting that the effect is tied to verifier-induced optimization pressure rather than to one inference interface. Applying

the same analysis to other domains such as SWE tasks and kernel generation requires first identifying a comparable ordered axis, such as test-suite strength or performance tolerance. The input-length thresholds are a coarse proxy for test-case scale and the optimization stress it induces, while our experiments show that it is a reliable proxy that consistently exposes the trade-off. Our ensemble comparisons match code generation count rather than token or wall-clock cost. This is most appropriate in settings where rollouts are easy to scale and malformed generations can be filtered and replaced, but matched-token or matched-wall-clock evaluation would be a stricter test. Appendix H gives weight-space analysis of the frontier: the endpoint difference is high-rank and spread across layers, while layer stitching experiments suggest that the behavioral control mainly comes from the middle layers. This leaves a more mechanistic version of the study open: one could train RL with explicit constraints, such as LoRA or frozen-layer variants, and test whether the frontier direction can be made more localized by construction.

## 7 Conclusion

Extrapolative weight averaging reveals that code RL checkpoints trained under nested verifier strictness lie on a correctness-efficiency frontier. On hard competitive-programming problems, stricter verification does not reliably increase solve rate; it rotates failures between inefficiency and incorrectness. Interpolation recovers this frontier, extrapolation extends it, and extrapolated checkpoints provide useful diversity for inference-time scaling. Moving beyond the frontier will likely require not only stricter tests or smoother scalar rewards, but training signals that reveal why programs fail and help models reduce semantic and computational failures together.

## Reproducibility Statement

All base models, training datasets, and evaluation benchmarks used in this work are publicly available, including Qwen 2.5 7B, CWM-SFT 32B, CodeContestsPlus, OpenCodeReasoning-2, OpenMathReasoning, and LiveCodeBench. We describe the training objectives, verifier thresholds, evaluation protocol, outcome taxonomy, tool-use curriculum, hyperparameters, and compute requirements in Section 2 and Appendix C; statistical procedures for reported confidence intervals and bootstrap estimates are described alongside the corresponding results. We do not release training code, model checkpoints, or new datasets, but the paper provides the experimental details needed to independently reconstruct the main settings from public assets.

## Acknowledgment

We thank Loïc Cabannes, Matteo Pagliardini, Fabian Gloeckle, Ori Yoran, Gautier Izacard, Keyur Muzumdar, David Zhang, Rémi Munos for all the fruitful discussion. We thank all the FAIR CodeGen team members for the support in the development of the project.

## References

- Wasi Uddin Ahmad, Somshubra Majumdar, Aleksander Ficek, Sean Narenthiran, Mehrzad Samadi, Jocelyn Huang, Siddhartha Jain, Vahid Noroozi, and Boris Ginsburg. Opencodereasoning-ii: A simple test time scaling approach via self-critique, 2025. <https://arxiv.org/abs/2507.09075>.
- Yuchen Cai, Ding Cao, Xin Xu, Zijun Yao, Yuqing Huang, Zhenyu Tan, Benyi Zhang, Guangzhong Sun, Guiquan Liu, and Junfeng Fang. On predictability of reinforcement learning dynamics for large language models, 2026. <https://arxiv.org/abs/2510.00553>.
- Pierre Chambon, Baptiste Roziere, Benoit Sagot, and Gabriel Synnaeve. Bigo(bench) – can llms generate code with controlled time and space complexity?, 2025. <https://arxiv.org/abs/2503.15242>.
- Ganqu Cui, Yuchen Zhang, Jiacheng Chen, Lifan Yuan, Zhi Wang, Yuxin Zuo, Haozhan Li, Yuchen Fan, Huayu Chen, Weize Chen, Zhiyuan Liu, Hao Peng, Lei Bai, Wanli Ouyang, Yu Cheng, Bowen Zhou, and Ning Ding. The entropy mechanism of reinforcement learning for reasoning language models, 2025. <https://arxiv.org/abs/2505.22617>.
- Ning Dai, Zheng Wu, Renjie Zheng, Ziyun Wei, Wenlei Shi, Xing Jin, Guanlin Liu, Chen Dun, Liang Huang, and Lin Yan. Process supervision-guided policy optimization for code generation, 2025. <https://arxiv.org/abs/2410.17621>.
- Mingzhe Du, Anh Tuan Luu, Bin Ji, Qian Liu, and See-Kiong Ng. Mercury: A code efficiency benchmark for code large language models. In Amir Globersons, Lester Mackey, Danielle Belgrave, Angela Fan, Ulrich Paquet, Jakub M. Tomczak, and Cheng Zhang, editors, *Advances in Neural Information Processing Systems 38: Annual Conference on Neural Information Processing Systems 2024, NeurIPS 2024, Vancouver, BC, Canada, December 10 - 15, 2024*, 2024. [http://papers.nips.cc/paper\\_files/paper/2024/hash/1df1df43b58845650b8dada00fca9772-Abstract-Datasets\\_and\\_Benchmarks\\_Track.html](http://papers.nips.cc/paper_files/paper/2024/hash/1df1df43b58845650b8dada00fca9772-Abstract-Datasets_and_Benchmarks_Track.html).
- Mingzhe Du, Luu Anh Tuan, Yue Liu, Yuhao Qing, Dong Huang, Xinyi He, Qian Liu, Zejun Ma, and See kiong Ng. Afterburner: Reinforcement learning facilitates self-improving code efficiency optimization, 2025. <https://arxiv.org/abs/2505.23387>.
- FAIR CodeGen team, Jade Copet, Quentin Carbonneaux, Gal Cohen, Jonas Gehring, Jacob Kahn, Jannik Kossen, Felix Kreuk, Emily McMilin, Michel Meyer, Yuxiang Wei, David Zhang, Kunhao Zheng, Jordi Armengol-Estapé, Pedram Bashiri, Maximilian Beck, Pierre Chambon, Abhishek Charnalia, Chris Cummins, Juliette Decugis, Zacharias V. Fisches, François Fleuret, Fabian Gloeckle, Alex Gu, Michael Hassid, Daniel Haziza, Badr Youbi Idrissi, Christian Keller, Rahul Kindi, Hugh Leather, Gallil Maimon, Aram Markosyan, Francisco Massa, Pierre-Emmanuel Mazaré, Vegard Mella, Naila Murray, Keyur Muzumdar, Peter O’Hearn, Matteo Pagliardini, Dmitrii Pedchenko, Tal Remez, Volker Seeker, Marco Selvi, Oren Sultan, Sida Wang, Luca Wehrstedt, Ori Yoran, Lingming Zhang, Taco Cohen, Yossi Adi, and Gabriel Synnaeve. Cwm: An open-weights llm for research on code generation with world models, 2025. <https://arxiv.org/abs/2510.02387>.
- Jonathan Frankle, Gintare Karolina Dziugaite, Daniel M. Roy, and Michael Carbin. Linear mode connectivity and the lottery ticket hypothesis. In *Proceedings of the 37th International Conference on Machine Learning, ICML 2020, 13-18 July 2020, Virtual Event*, Proceedings of Machine Learning Research, pages 3259–3269. PMLR, 2020. <http://proceedings.mlr.press/v119/frankle20a.html>.
- Yulu Gan and Phillip Isola. Neural thickets: Diverse task experts are dense around pretrained weights, 2026. <https://arxiv.org/abs/2603.12228>.
- Jonas Gehring, Kunhao Zheng, Jade Copet, Vegard Mella, Taco Cohen, and Gabriel Synnaeve. RLEF: grounding code llms in execution feedback with reinforcement learning. In Aarti Singh, Maryam Fazel, Daniel Hsu, Simon Lacoste-Julien, Felix Berkenkamp, Tegan Maharaj, Kiri Wagstaff, and Jerry Zhu, editors, *Forty-second International Conference on Machine Learning, ICML 2025, Vancouver, BC, Canada, July 13-19, 2025*, Proceedings of Machine Learning Research. PMLR / OpenReview.net, 2025. <https://proceedings.mlr.press/v267/gehring25a.html>.
- Daya Guo, Dejian Yang, Haowei Zhang, Junxiao Song, Peiyi Wang, Qihao Zhu, Runxin Xu, Ruoyu Zhang, Shirong Ma, Xiao Bi, Xiaokang Zhang, Xingkai Yu, Yu Wu, Z. F. Wu, Zhibin Gou, Zhihong Shao, Zhuoshu Li, Ziyi Gao, Aixin Liu, Bing Xue, Bingxuan Wang, Bochao Wu, Bei Feng, Chengda Lu, Chenggang Zhao, Chengqi Deng, Chong Ruan, Damai Dai, Deli Chen, Dongjie Ji, Erhang Li, Fangyun Lin, Fucong Dai, Fuli Luo, Guangbo Hao, Guanting Chen, Guowei Li, H. Zhang, Hanwei Xu, Honghui Ding, Huazuo Gao, Hui Qu, Hui Li, Jianzhong Guo, Jiashi Li, Jingchang Chen, Jingyang Yuan, Jinhao Tu, Junjie Qiu, Junlong Li, J. L. Cai, Jiaqi Ni, Jian Liang, Jin Chen, Kai Dong, Kai Hu, Kaichao You, Kaige Gao, Kang Guan, Kexin Huang, Kuai Yu, Lean Wang, Lecong Zhang, Liang Zhao, Litong Wang, Liyue Zhang, Lei Xu, Leyi Xia, Mingchuan Zhang, Minghua Zhang, Minghui Tang, Mingxu Zhou, Meng Li, Miaojun Wang, Mingming Li, Ning Tian, Panpan Huang, Peng Zhang, Qiancheng Wang, Qinyu

- Chen, Qiushi Du, Ruiqi Ge, Ruisong Zhang, Ruizhe Pan, Runji Wang, R. J. Chen, R. L. Jin, Ruyi Chen, Shanghao Lu, Shangyan Zhou, Shanhuang Chen, Shengfeng Ye, Shiyu Wang, Shuiping Yu, Shunfeng Zhou, Shuting Pan, S. S. Li, Shuang Zhou, Shaoqing Wu, Tao Yun, Tian Pei, Tianyu Sun, T. Wang, Wangding Zeng, Wen Liu, Wenfeng Liang, Wenjun Gao, Wenqin Yu, Wentao Zhang, W. L. Xiao, Wei An, Xiaodong Liu, Xiaohan Wang, Xiaokang Chen, Xiaotao Nie, Xin Cheng, Xin Liu, Xin Xie, Xingchao Liu, Xinyu Yang, Xinyuan Li, Xuecheng Su, Xuheng Lin, X. Q. Li, Xiangyue Jin, Xiaojin Shen, Xiaosha Chen, Xiaowen Sun, Xiaoxiang Wang, Xinnan Song, Xinyi Zhou, Xianzu Wang, Xinxia Shan, Y. K. Li, Y. Q. Wang, Y. X. Wei, Yang Zhang, Yanhong Xu, Yao Li, Yao Zhao, Yaofeng Sun, Yaohui Wang, Yi Yu, Yichao Zhang, Yifan Shi, Yiliang Xiong, Ying He, Yishi Piao, Yisong Wang, Yixuan Tan, Yiyang Ma, Yiyuan Liu, Yongqiang Guo, Yuan Ou, Yudian Wang, Yue Gong, Yuheng Zou, Yujia He, Yunfan Xiong, Yuxiang Luo, Yuxiang You, Yuxuan Liu, Yuyang Zhou, Y. X. Zhu, Yanping Huang, Yaohui Li, Yi Zheng, Yuchen Zhu, Yunxian Ma, Ying Tang, Yukun Zha, Yuting Yan, Z. Z. Ren, Zehui Ren, Zhangli Sha, Zhe Fu, Zhean Xu, Zhenda Xie, Zhengyan Zhang, Zhewen Hao, Zhicheng Ma, Zhigang Yan, Zhiyu Wu, Zihui Gu, Zijia Zhu, Zijun Liu, Zilin Li, Ziwei Xie, Ziyang Song, Zizheng Pan, Zhen Huang, Zhipeng Xu, Zhongyu Zhang, and Zhen Zhang. Deepseek-r1 incentivizes reasoning in llms through reinforcement learning. *Nature*, 645(8081):633–638, Sept 2025. ISSN 1476-4687. doi: 10.1038/s41586-025-09422-z. <http://dx.doi.org/10.1038/s41586-025-09422-z>.
- Dan Hendrycks, Steven Basart, Saurav Kadavath, Mantas Mazeika, Akul Arora, Ethan Guo, Collin Burns, Samir Puranik, Horace He, Dawn Song, and Jacob Steinhardt. Measuring coding challenge competence with APPS. In Joaquin Vanschoren and Sai-Kit Yeung, editors, *Proceedings of the Neural Information Processing Systems Track on Datasets and Benchmarks 1, NeurIPS Datasets and Benchmarks 2021, December 2021, virtual*, 2021. <https://datasets-benchmarks-proceedings.neurips.cc/paper/2021/hash/c24cd76e1ce41366a4bbe8a49b02a028-Abstract-round2.html>.
- Dong Huang, Yuhao Qing, Weiyi Shang, Heming Cui, and Jie Zhang. Effibench: Benchmarking the efficiency of automatically generated code. In Amir Globersons, Lester Mackey, Danielle Belgrave, Angela Fan, Ulrich Paquet, Jakub M. Tomczak, and Cheng Zhang, editors, *Advances in Neural Information Processing Systems 38: Annual Conference on Neural Information Processing Systems 2024, NeurIPS 2024, Vancouver, BC, Canada, December 10 - 15, 2024*, 2024. [http://papers.nips.cc/paper\\_files/paper/2024/hash/15807b6e09d691fe5e96cdecde6d7b80-Abstract-Datasets\\_and\\_Benchmarks\\_Track.html](http://papers.nips.cc/paper_files/paper/2024/hash/15807b6e09d691fe5e96cdecde6d7b80-Abstract-Datasets_and_Benchmarks_Track.html).
- Gabriel Ilharco, Marco Túlio Ribeiro, Mitchell Wortsman, Ludwig Schmidt, Hannaneh Hajishirzi, and Ali Farhadi. Editing models with task arithmetic. In *The Eleventh International Conference on Learning Representations, ICLR 2023, Kigali, Rwanda, May 1-5, 2023*. OpenReview.net, 2023. <https://openreview.net/forum?id=6t0Kwf8-jrj>.
- Naman Jain, King Han, Alex Gu, Wen-Ding Li, Fanjia Yan, Tianjun Zhang, Sida Wang, Armando Solar-Lezama, Koushik Sen, and Ion Stoica. Livecodebench: Holistic and contamination free evaluation of large language models for code. In *The Thirteenth International Conference on Learning Representations, ICLR 2025, Singapore, April 24-28, 2025*. OpenReview.net, 2025. <https://openreview.net/forum?id=chfJJYC3iL>.
- Yiyang Jin, Kunzhao Xu, Hang Li, Xueting Han, Yanmin Zhou, Cheng Li, and Jing Bai. Reveal: Self-evolving code agents via reliable self-verification, 2025. <https://arxiv.org/abs/2506.11442>.
- Joongwon Kim, Wannan Yang, Kelvin Niu, Hongming Zhang, Yun Zhu, Eryk Helenowski, Ruan Silva, Zhengxing Chen, Srinivasan Iyer, Manzil Zaheer, Daniel Fried, Hannaneh Hajishirzi, Sanjeev Arora, Gabriel Synnaeve, Ruslan Salakhutdinov, and Anirudh Goyal. Scaling test-time compute for agentic coding, 2026. <https://arxiv.org/abs/2604.16529>.
- Kimi Team, Yifan Bai, Yiping Bao, Y. Charles, Cheng Chen, Guanduo Chen, Haiting Chen, Huarong Chen, Jiahao Chen, Ningxin Chen, Ruijue Chen, Yanru Chen, Yuankun Chen, Yutian Chen, Zhuofu Chen, Jialei Cui, Hao Ding, Mengnan Dong, Angang Du, Chenzhuang Du, Dikang Du, Yulun Du, Yu Fan, Yichen Feng, Kelin Fu, Bofei Gao, Chenxiao Gao, Hongcheng Gao, Peizhong Gao, Tong Gao, Yuyao Ge, Shangyi Geng, Qizheng Gu, Xinran Gu, Longyu Guan, Haiqing Guo, Jianhang Guo, Xiaoru Hao, Tianhong He, Weiran He, Wenyang He, Yunjia He, Chao Hong, Hao Hu, Yangyang Hu, Zhenxing Hu, Weixiao Huang, Zhiqi Huang, Zihao Huang, Tao Jiang, Zhejun Jiang, Xinyi Jin, Yongsheng Kang, Guokun Lai, Cheng Li, Fang Li, Haoyang Li, Ming Li, Wentao Li, Yang Li, Yanhao Li, Yiwei Li, Zhaowei Li, Zheming Li, Hongzhan Lin, Xiaohan Lin, Zongyu Lin, Chengyin Liu, Chenyu Liu, Hongzhang Liu, Jingyuan Liu, Junqi Liu, Liang Liu, Shaowei Liu, T. Y. Liu, Tianwei Liu, Weizhou Liu, Yangyang Liu, Yibo Liu, Yiping Liu, Yue Liu, Zhengying Liu, Enzhe Lu, Haoyu Lu, Lijun Lu, Yashuo Luo, Shengling Ma, Xinyu Ma, Yingwei Ma, Shaoguang Mao, Jie Mei, Xin Men, Yibo Miao, Siyuan Pan, Yebo Peng, Ruoyu Qin, Zeyu Qin, Bowen Qu, Zeyu Shang, Lidong Shi, Shengyuan Shi, Feifan Song, Jianlin Su, Zhengyuan Su, Lin Sui, Xinjie Sun, Flood Sung, Yunpeng Tai, Heyi Tang, Jiawen Tao, Qifeng Teng, Chaoran Tian, Chensi Wang, Dinglu Wang, Feng Wang, Hailong Wang, Haiming Wang, Jianzhou Wang, Jiayang Wang, Jinhong Wang, Shengjie Wang, Shuyi Wang, Si Wang, Xinyuan Wang, Yao Wang, Yejie Wang, Yiqin Wang, Yuxin Wang, Yuzhi Wang, Zhaoji Wang, Zhengtao Wang, Zhengtao Wang, Zhexu Wang, Chu Wei, Qianqian Wei, Haoning Wu, Wenhao Wu, Xingzhe Wu,

- Yuxin Wu, Chenjun Xiao, Jin Xie, Xiaotong Xie, Weimin Xiong, Boyu Xu, Jinjing Xu, L. H. Xu, Lin Xu, Suting Xu, Weixin Xu, Xinran Xu, Yangchuan Xu, Ziyao Xu, Jing Xu, Junjie Yan, Yuzi Yan, Hao Yang, Xiaofei Yang, Yi Yang, Ying Yang, Zhen Yang, Zhilin Yang, Zonghan Yang, Haotian Yao, Xingcheng Yao, Wenjie Ye, Zhuorui Ye, Bohong Yin, Longhui Yu, Enming Yuan, Hongbang Yuan, Mengjie Yuan, Siyu Yuan, Haobing Zhan, Dehao Zhang, Hao Zhang, Wanlu Zhang, Xiaobin Zhang, Yadong Zhang, Yangkun Zhang, Yichi Zhang, Yizhi Zhang, Yongting Zhang, Yu Zhang, Yutao Zhang, Yutong Zhang, Zheng Zhang, Haotian Zhao, Yikai Zhao, Zijia Zhao, Huabin Zheng, Shaojie Zheng, Longguang Zhong, Jianren Zhou, Xinyu Zhou, Zaida Zhou, Jinguo Zhu, Zhen Zhu, Weiyu Zhuang, and Xinxing Zu. Kimi k2: Open agentic intelligence, 2026. <https://arxiv.org/abs/2507.20534>.
- Dacheng Li, Shiyi Cao, Chengkun Cao, Xiuyu Li, Shangyin Tan, Kurt Keutzer, Jiarong Xing, Joseph E. Gonzalez, and Ion Stoica. S\*: Test time scaling for code generation. In Christos Christodoulopoulos, Tanmoy Chakraborty, Carolyn Rose, and Violet Peng, editors, *Findings of the Association for Computational Linguistics: EMNLP 2025, Suzhou, China, November 4-9, 2025*, pages 15964–15978. Association for Computational Linguistics, 2025a. <https://aclanthology.org/2025.findings-emnlp.865/>.
- Qingyao Li, Xinyi Dai, Xiangyang Li, Weinan Zhang, Yasheng Wang, Ruiming Tang, and Yong Yu. CodePRM: Execution feedback-enhanced process reward model for code generation. In Wanxiang Che, Joyce Nabende, Ekaterina Shutova, and Mohammad Taher Pilehvar, editors, *Findings of the Association for Computational Linguistics: ACL 2025*, pages 8169–8182, Vienna, Austria, July 2025b. Association for Computational Linguistics. ISBN 979-8-89176-256-5. doi: 10.18653/v1/2025.findings-acl.428. <https://aclanthology.org/2025.findings-acl.428/>.
- Rongao Li, Jie Fu, Bo-Wen Zhang, Tao Huang, Zhihong Sun, Chen Lyu, Guang Liu, Zhi Jin, and Ge Li. Taco: Topics in algorithmic code generation dataset, 2023. <https://arxiv.org/abs/2312.14852>.
- Yujia Li, David Choi, Junyoung Chung, Nate Kushman, Julian Schrittwieser, Rémi Leblond, Tom Eccles, James Keeling, Felix Gimeno, Agustin Dal Lago, Thomas Hubert, Peter Choy, Cyprien de Masson d’Autume, Igor Babuschkin, Xinyun Chen, Po-Sen Huang, Johannes Welbl, Sven Gowal, Alexey Cherepanov, James Molloy, Daniel J. Mankowitz, Esme Sutherland Robson, Pushmeet Kohli, Nando de Freitas, Koray Kavukcuoglu, and Oriol Vinyals. Competition-level code generation with alphacode. *Science*, 378(6624):1092–1097, December 2022. ISSN 1095-9203. doi: 10.1126/science.abq1158. <http://dx.doi.org/10.1126/science.abq1158>.
- Yong Lin, Hangyu Lin, Wei Xiong, Shizhe Diao, Jianmeng Liu, Jipeng Zhang, Rui Pan, Haoxiang Wang, Wenbin Hu, Hanning Zhang, Hanze Dong, Renjie Pi, Han Zhao, Nan Jiang, Heng Ji, Yuan Yao, and Tong Zhang. Mitigating the alignment tax of RLHF. In Yaser Al-Onaizan, Mohit Bansal, and Yun-Nung Chen, editors, *Proceedings of the 2024 Conference on Empirical Methods in Natural Language Processing, EMNLP 2024, Miami, FL, USA, November 12-16, 2024*, pages 580–606. Association for Computational Linguistics, 2024. doi: 10.18653/V1/2024.EMNLP-MAIN.35. <https://doi.org/10.18653/v1/2024.emnlp-main.35>.
- Jiawei Liu, Chunqiu Steven Xia, Yuyao Wang, and Lingming Zhang. Is your code generated by chatgpt really correct? rigorous evaluation of large language models for code generation. In Alice Oh, Tristan Naumann, Amir Globerson, Kate Saenko, Moritz Hardt, and Sergey Levine, editors, *Advances in Neural Information Processing Systems 36: Annual Conference on Neural Information Processing Systems 2023, NeurIPS 2023, New Orleans, LA, USA, December 10 - 16, 2023*, 2023. [http://papers.nips.cc/paper\\_files/paper/2023/hash/43e9d647ccd3e4b7b5baab53f0368686-Abstract-Conference.html](http://papers.nips.cc/paper_files/paper/2023/hash/43e9d647ccd3e4b7b5baab53f0368686-Abstract-Conference.html).
- Zichen Liu, Changyu Chen, Wenjun Li, Penghui Qi, Tianyu Pang, Chao Du, Wee Sun Lee, and Min Lin. Understanding r1-zero-like training: A critical perspective, 2025. <https://arxiv.org/abs/2503.20783>.
- Jeffrey Jian Ma, Milad Hashemi, Amir Yazdanbakhsh, Kevin Swersky, Ofir Press, Enhui Li, Vijay Janapa Reddi, and Parthasarathy Ranganathan. Swe-fficiency: Can language models optimize real-world repositories on real workloads?, 2025. <https://arxiv.org/abs/2511.06090>.
- Gallil Maimon, Ori Yoran, Felix Kreuk, Michael Hassid, Gal Cohen, Pierre Chambon, and Yossi Adi. Self-execution simulation improves coding models, 2026. <https://arxiv.org/abs/2604.03253>.
- MiniMax, :, Aili Chen, Aonian Li, Bangwei Gong, Binyang Jiang, Bo Fei, Bo Yang, Boji Shan, Changqing Yu, Chao Wang, Cheng Zhu, Chengjun Xiao, Chengyu Du, Chi Zhang, Chu Qiao, Chunhao Zhang, Chunhui Du, Congchao Guo, Da Chen, Deming Ding, Dianjun Sun, Dong Li, Enwei Jiao, Haigang Zhou, Haimo Zhang, Han Ding, Haohai Sun, Haoyu Feng, Huaiguang Cai, Haichao Zhu, Jian Sun, Jiaqi Zhuang, Jiaren Cai, Jiayuan Song, Jin Zhu, Jingyang Li, Jinhao Tian, Jinli Liu, Junhao Xu, Junjie Yan, Junteng Liu, Junxian He, Kaiyi Feng, Ke Yang, Kecheng Xiao, Le Han, Leyang Wang, Lianfei Yu, Liheng Feng, Lin Li, Lin Zheng, Linge Du, Lingyu Yang, Lunbin Zeng, Minghui Yu, Mingliang Tao, Mingyuan Chi, Mozhi Zhang, Mujie Lin, Nan Hu, Nongyu Di, Peng Gao, Pengfei Li, Pengyu Zhao, Qibing Ren, Qidi Xu, Qile Li, Qin Wang, Rong Tian, Ruitao Leng, Shaoxiang Chen, Shaoyu Chen, Shengmin Shi, Shitong Weng, Shuchang Guan, Shuqi Yu, Sichen Li, Songquan Zhu, Tengfei Li, Tianchi Cai,

- Tianrun Liang, Weiyu Cheng, Weize Kong, Wenkai Li, Xiancai Chen, Xiangjun Song, Xiao Luo, Xiao Su, Xiaobo Li, Xiaodong Han, Xinzhu Hou, Xuan Lu, Xun Zou, Xuyang Shen, Yan Gong, Yan Ma, Yang Wang, Yiqi Shi, Yiran Zhong, Yonghong Duan, Yongxiang Fu, Yongyi Hu, Yu Gao, Yuanxiang Fan, Yufeng Yang, Yuhao Li, Yulin Hu, Yunan Huang, Yunji Li, Yunzhi Xu, Yuxin Mao, Yuxuan Shi, Yuze Wenren, Zehan Li, Zelin Li, Zhanxu Tian, Zhengmao Zhu, Zhenhua Fan, Zhenzhen Wu, Zhichao Xu, Zhihang Yu, Zhiheng Lyu, Zhuo Jiang, Zibo Gao, Zijia Wu, Zijian Song, and Zijun Sun. Minimax-m1: Scaling test-time compute efficiently with lightning attention, 2025. <https://arxiv.org/abs/2506.13585>.
- Ivan Moshkov, Darragh Hanley, Ivan Sorokin, Shubham Toshniwal, Christof Henkel, Benedikt Schifferer, Wei Du, and Igor Gitman. Aimo-2 winning solution: Building state-of-the-art mathematical reasoning models with openmathreasoning dataset, 2025. <https://arxiv.org/abs/2504.16891>.
- Anne Ouyang, Simon Guo, Simran Arora, Alex L. Zhang, William Hu, Christopher Ré, and Azalia Mirhoseini. Kernelbench: Can llms write efficient GPU kernels? In Aarti Singh, Maryam Fazel, Daniel Hsu, Simon Lacoste-Julien, Felix Berkenkamp, Tegan Maharaj, Kiri Wagstaff, and Jerry Zhu, editors, *Forty-second International Conference on Machine Learning, ICML 2025, Vancouver, BC, Canada, July 13-19, 2025*, Proceedings of Machine Learning Research. PMLR / OpenReview.net, 2025. <https://proceedings.mlr.press/v267/ouyang25a.html>.
- Qwen, :, An Yang, Baosong Yang, Beichen Zhang, Binyuan Hui, Bo Zheng, Bowen Yu, Chengyuan Li, Dayiheng Liu, Fei Huang, Haoran Wei, Huan Lin, Jian Yang, Jianhong Tu, Jianwei Zhang, Jianxin Yang, Jiayi Yang, Jingren Zhou, Junyang Lin, Kai Dang, Keming Lu, Keqin Bao, Kexin Yang, Le Yu, Mei Li, Mingfeng Xue, Pei Zhang, Qin Zhu, Rui Men, Runji Lin, Tianhao Li, Tianyi Tang, Tingyu Xia, Xingzhang Ren, Xuancheng Ren, Yang Fan, Yang Su, Yichang Zhang, Yu Wan, Yuqiong Liu, Zeyu Cui, Zhenru Zhang, and Zihan Qiu. Qwen2.5 technical report, 2025. <https://arxiv.org/abs/2412.15115>.
- Alexandre Ramé, Guillaume Couairon, Corentin Dancette, Jean-Baptiste Gaya, Mustafa Shukor, Laure Soulier, and Matthieu Cord. Rewarded soups: towards pareto-optimal alignment by interpolating weights fine-tuned on diverse rewards. In Alice Oh, Tristan Naumann, Amir Globerson, Kate Saenko, Moritz Hardt, and Sergey Levine, editors, *Advances in Neural Information Processing Systems 36: Annual Conference on Neural Information Processing Systems 2023, NeurIPS 2023, New Orleans, LA, USA, December 10 - 16, 2023*, 2023. [http://papers.nips.cc/paper\\_files/paper/2023/hash/e12a3b98b67e8395f639fde4c2b03168-Abstract-Conference.html](http://papers.nips.cc/paper_files/paper/2023/hash/e12a3b98b67e8395f639fde4c2b03168-Abstract-Conference.html).
- Alexandre Ramé, Nino Vieillard, Léonard Hussenot, Robert Dadashi, Geoffrey Cideron, Olivier Bachem, and Johan Ferret. WARM: on the benefits of weight averaged reward models. In Ruslan Salakhutdinov, Zico Kolter, Katherine A. Heller, Adrian Weller, Nuria Oliver, Jonathan Scarlett, and Felix Berkenkamp, editors, *Forty-first International Conference on Machine Learning, ICML 2024, Vienna, Austria, July 21-27, 2024*, Proceedings of Machine Learning Research, pages 42048–42073. PMLR / OpenReview.net, 2024. <https://proceedings.mlr.press/v235/rame24a.html>.
- Alexandre Ramé, Johan Ferret, Nino Vieillard, Robert Dadashi, Léonard Hussenot, Pierre-Louis Cedoz, Pier Giuseppe Sessa, Sertan Girgin, Arthur Douillard, and Olivier Bachem. Warp: On the benefits of weight averaged rewarded policies, 2024. <https://arxiv.org/abs/2406.16768>.
- Yunhao Tang, Kunhao Zheng, Gabriel Synnaeve, and Rémi Munos. Optimizing language models for inference time objectives using reinforcement learning. In Aarti Singh, Maryam Fazel, Daniel Hsu, Simon Lacoste-Julien, Felix Berkenkamp, Tegan Maharaj, Kiri Wagstaff, and Jerry Zhu, editors, *Forty-second International Conference on Machine Learning, ICML 2025, Vancouver, BC, Canada, July 13-19, 2025*, Proceedings of Machine Learning Research. PMLR / OpenReview.net, 2025. <https://proceedings.mlr.press/v267/tang25o.html>.
- Alexandre Verine, Florian Le Bronnec, Kunhao Zheng, Alexandre Allauzen, Yann Chevaleyre, and Benjamin Négrevigne. Improving diversity in language models: When temperature fails, change the loss. In Aarti Singh, Maryam Fazel, Daniel Hsu, Simon Lacoste-Julien, Felix Berkenkamp, Tegan Maharaj, Kiri Wagstaff, and Jerry Zhu, editors, *Forty-second International Conference on Machine Learning, ICML 2025, Vancouver, BC, Canada, July 13-19, 2025*, Proceedings of Machine Learning Research. PMLR / OpenReview.net, 2025. <https://proceedings.mlr.press/v267/verine25a.html>.
- Siddhant Waghjale, Vishruth Veerendranath, Zhiruo Wang, and Daniel Fried. ECCO: can we improve model-generated code efficiency without sacrificing functional correctness? In Yaser Al-Onaizan, Mohit Bansal, and Yun-Nung Chen, editors, *Proceedings of the 2024 Conference on Empirical Methods in Natural Language Processing, EMNLP 2024, Miami, FL, USA, November 12-16, 2024*, pages 15362–15376. Association for Computational Linguistics, 2024. doi: 10.18653/V1/2024.EMNLP-MAIN.859. <https://doi.org/10.18653/v1/2024.emnlp-main.859>.
- Ke Wang, Nikolaos Dimitriadis, Guillermo Ortiz-Jiménez, François Fleuret, and Pascal Frossard. Localizing task information for improved model merging and compression. In Ruslan Salakhutdinov, Zico Kolter, Katherine A. Heller, Adrian Weller, Nuria Oliver, Jonathan Scarlett, and Felix Berkenkamp, editors, *Forty-first International*

- Conference on Machine Learning, ICML 2024, Vienna, Austria, July 21-27, 2024*, Proceedings of Machine Learning Research, pages 50268–50287. PMLR / OpenReview.net, 2024. <https://proceedings.mlr.press/v235/wang24k.html>.
- Tianle Wang, Jiayu Liu, Zhongyuan Wu, Shenghao Jin, Wei Chen, Hao Xu, and Ning Miao. Linear dynamics in the rlvr training of large language models, 2026. <https://arxiv.org/abs/2601.04537>.
- Zihan Wang, Siyao Liu, Yang Sun, Hongyan Li, and Kai Shen. Codecontests+: High-quality test case generation for competitive programming, 2025. <https://arxiv.org/abs/2506.05817>.
- Mitchell Wortsman, Gabriel Ilharco, Samir Yitzhak Gadre, Rebecca Roelofs, Raphael Gontijo Lopes, Ari S. Morcos, Hongseok Namkoong, Ali Farhadi, Yair Carmon, Simon Kornblith, and Ludwig Schmidt. Model soups: averaging weights of multiple fine-tuned models improves accuracy without increasing inference time. In Kamalika Chaudhuri, Stefanie Jegelka, Le Song, Csaba Szepesvári, Gang Niu, and Sivan Sabato, editors, *International Conference on Machine Learning, ICML 2022, 17-23 July 2022, Baltimore, Maryland, USA*, Proceedings of Machine Learning Research, pages 23965–23998. PMLR, 2022. <https://proceedings.mlr.press/v162/wortsman22a.html>.
- Fang Wu, Weihao Xuan, Ximing Lu, Mingjie Liu, Yi Dong, Zaid Harchaoui, and Yejin Choi. The invisible leash: Why rlvr may or may not escape its origin, 2026. <https://arxiv.org/abs/2507.14843>.
- Zhenghai Xue, Longtao Zheng, Qian Liu, Yingru Li, Xiaosen Zheng, Zejun Ma, and Bo An. Simpletir: End-to-end reinforcement learning for multi-turn tool-integrated reasoning, 2025. <https://arxiv.org/abs/2509.02479>.
- Enneng Yang, Zhenyi Wang, Li Shen, Shiwei Liu, Guibing Guo, Xingwei Wang, and Dacheng Tao. Adamerging: Adaptive model merging for multi-task learning. In *The Twelfth International Conference on Learning Representations, ICLR 2024, Vienna, Austria, May 7-11, 2024*. OpenReview.net, 2024. <https://openreview.net/forum?id=nZP6NgD3QY>.
- Qiyang Yu, Zheng Zhang, Ruofei Zhu, Yufeng Yuan, Xiaochen Zuo, Yu Yue, Weinan Dai, Tiantian Fan, Gaohong Liu, Lingjun Liu, Xin Liu, Haibin Lin, Zhiqi Lin, Bole Ma, Guangming Sheng, Yuxuan Tong, Chi Zhang, Mofan Zhang, Wang Zhang, Hang Zhu, Jinhua Zhu, Jiaze Chen, Jiangjie Chen, Chengyi Wang, Hongli Yu, Yuxuan Song, Xiangpeng Wei, Hao Zhou, Jingjing Liu, Wei-Ying Ma, Ya-Qin Zhang, Lin Yan, Mu Qiao, Yonghui Wu, and Mingxuan Wang. Dapo: An open-source llm reinforcement learning system at scale, 2025. <https://arxiv.org/abs/2503.14476>.
- Yang Yue, Zhiqi Chen, Rui Lu, Andrew Zhao, Zhaokai Wang, Yang Yue, Shiji Song, and Gao Huang. Does reinforcement learning really incentivize reasoning capacity in llms beyond the base model?, 2025. <https://arxiv.org/abs/2504.13837>.
- Chujie Zheng, Ziqi Wang, Heng Ji, Minlie Huang, and Nanyun Peng. Model extrapolation expedites alignment. In Wanxiang Che, Joyce Nabende, Ekaterina Shutova, and Mohammad Taher Pilehvar, editors, *Proceedings of the 63rd Annual Meeting of the Association for Computational Linguistics (Volume 1: Long Papers), ACL 2025, Vienna, Austria, July 27 - August 1, 2025*, pages 1025–1041. Association for Computational Linguistics, 2025a. <https://aclanthology.org/2025.acl-long.51/>.
- Kunhao Zheng, Juliette Decugis, Jonas Gehring, Taco Cohen, Benjamin NéXuanjinggrevergne, and Gabriel Synnaeve. What makes large language models reason in (multi-turn) code generation? In *The Thirteenth International Conference on Learning Representations, ICLR 2025, Singapore, April 24-28, 2025*. OpenReview.net, 2025b. <https://openreview.net/forum?id=Zk9guO19NS>.

# Appendix

## A A Second Weight-Space Frontier: Pass@1 vs Pass@ $k$ Performance

The main experiments use nested verifier coverage to create a controlled correctness-efficiency axis. To test whether the weight-averaging geometry is specific to that axis, we ran an auxiliary experiment between two RL checkpoints, trained from the same initialization (the SFT checkpoint from Qwen 2.5 7B as described in main text) but optimized for different sampling behavior. The firstll is trained using standard GRPO which exhibits stronger pass@1, and the second is trained under pass@8 objective as shown in Tang et al. (2025). We form interpolation and extrapolation checkpoints:

$$\theta_\alpha = \alpha \theta_{p@8} + (1 - \alpha) \theta_{p@1},$$

and evaluate checkpoints for  $\alpha \in [-0.5, 1.5]$  on LCB v5 + v6 (20240801-20250501), 454 problems in total, with temperature 1.0 and 200 samples per prompt.

**Interpolation produces a smooth behavioral frontier.** Figure 10 shows that interpolation traces a smooth curve in pass@1/pass@100 space. We follow the Precision/Recall framework (Verine et al., 2025) which uses pass@1 as a proxy for Precision, and pass@100 - pass@1 as a measure for Recall. Moving along the curve changes both the Precision (pass@1) and the Recall (pass@100 - pass@1). This confirms that the interpolation direction captures a meaningful behavioral axis even when the endpoints differ by training objective rather than by verifier coverage. Extrapolation is stable near the endpoints but gives diminishing returns: the most extreme extrapolated checkpoints ( $\alpha = -0.5, \alpha = 1.5$ ) degrade on both pass@1 and pass@100.

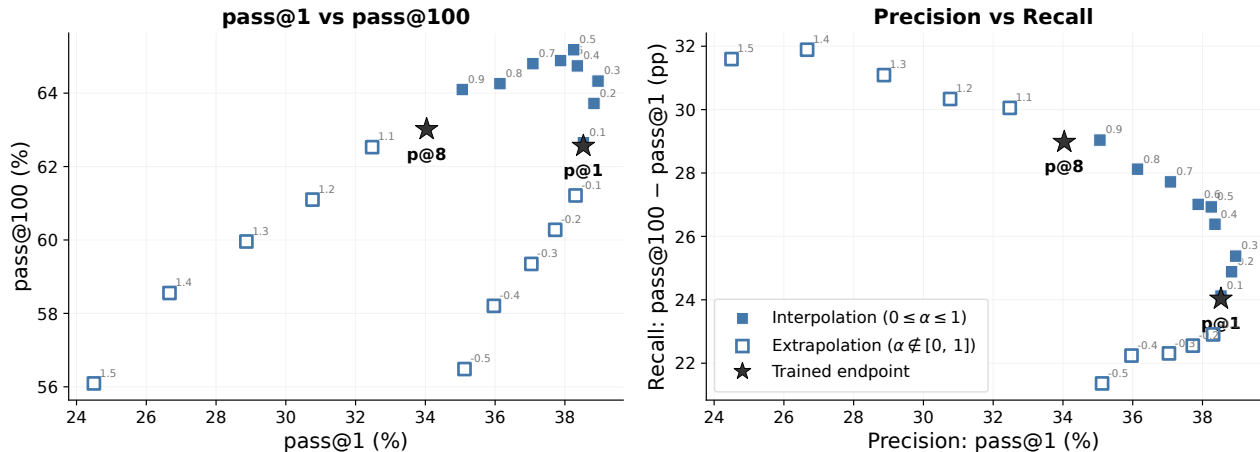


**Figure 10 A second weight-space frontier: pass@1 vs pass@100.** We average a pass@1-oriented endpoint (p@1,  $\alpha=0$ ) and a pass@8-oriented endpoint (p@8,  $\alpha=1$ ). **Left:** Interpolation traces a smooth curve in pass@1/pass@100 space; extrapolation remains locally meaningful but degrades at extreme values. **Right:** In the Precision/Recall view, sampling headroom peaks in the interpolation region, indicating that interpolated checkpoints have the most untapped potential under larger sampling budgets.

**Checkpoint banks exploit solved-set diversity.** As in the verifier-coverage frontier, nearby values of  $\alpha$  solve overlapping but distinct problem sets (Figure 11). This turnover can be exploited by checkpoint banks. Figure 12 shows that five-checkpoint banks with 200 samples each outperform either single endpoint with 1000 samples at pass@ $k$  for  $k \geq 10$ , reaching +3.5% on all problems and +5.4% on hard at pass@1000. Including one extrapolated checkpoint ( $\alpha=-0.2$ ) adds marginal diversity on hard problems: it uniquely solves 7 hard problems that no interpolation checkpoint covers. Conversely, 12 problems are uniquely solved by interpolation (6 hard, 6 medium), so extrapolation trades medium-difficulty coverage for hard-problem diversity: precisely the frontier exploration that weight averaging exposes.

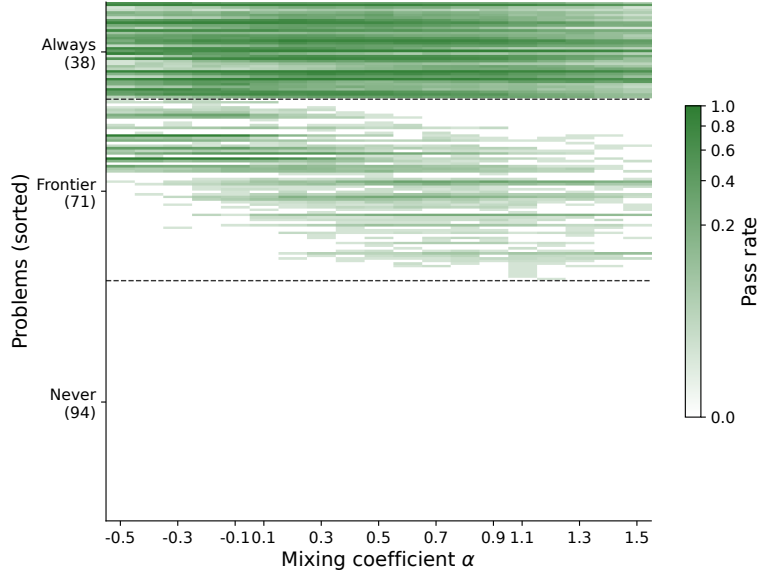


**Figure 11** Solved-set turnover along the interpolation axis of pass@1-trained checkpoint and pass@8-trained checkpoint (LCB/hard). Each row is one problem; columns are  $\alpha$  values. Unlike the main-text heatmap (Figure 7), which uses a linear color scale, we apply a power-law normalization ( $\gamma=0.3$ ) to highlight problems solved at low pass rates. Of 203 hard problems, 38 are always solved, 94 are never solved, and 71 frontier problems change solvability with  $\alpha$ , providing the diversity that checkpoint banks exploit.

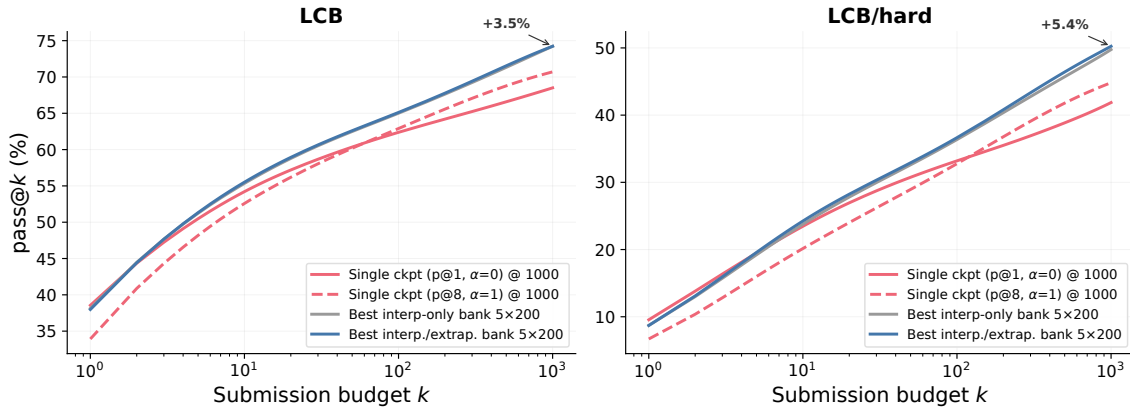


**Figure 12 Matched-budget checkpoint banks on LCB.** **Left:** On all problems, interpolation-only and interpolation/extrapolation banks overlap, both outperforming single-checkpoint sampling by +3.5% at pass@1000. **Right:** On hard problems, including an extrapolated checkpoint edges out interpolation-only by  $\sim 0.5\%$ , trading medium-difficulty coverage for hard-problem diversity.

**Scope and caveats.** We treat this experiment as supportive but not primary evidence. Unlike the nested verifier sweep, this setting is not a controlled sweep over a single monotone reward family, and the endpoints differ in both objective and training stage. Its role is to suggest that the frontier-navigation view can extend beyond correctness–efficiency, not to replace the controlled evidence in the main paper.

## B Seed Variance Analysis

To quantify the statistical reliability of our main findings, we repeat the pure-reasoning RL runs for each of the three coverage thresholds ( $\text{Keep} \leq 10^3$ ,  $\text{Keep} \leq 10^5$ , and All tests) with three independent random seeds at both the 7B and 32B model scales, and report mean  $\pm$  one standard deviation.

**Pass@1 stability.** Figure 13 shows the LCB pass@1 training curves across seeds. At the 32B scale, all three thresholds exhibit tight variance bands throughout training, with standard deviations below 0.5% at step 6k (e.g.  $\text{Keep} \leq 10^3$ :  $61.7 \pm 0.5\%$ ; All tests:  $61.6 \pm 0.2\%$ ). The 7B runs show moderately larger variance ( $\sim 0.7\text{-}1.0\%$ ), consistent with smaller models being more sensitive to initialization, but the relative ordering among thresholds is preserved across all seeds.

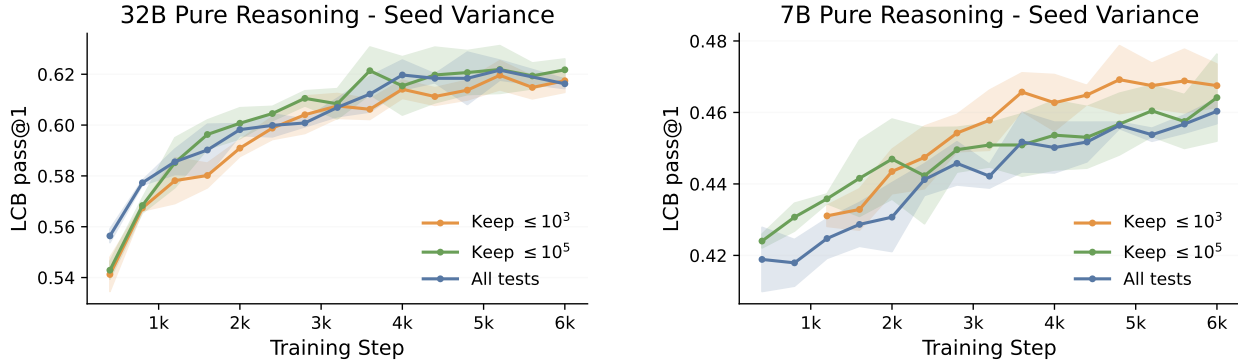


**Figure 13** Pass@1 on LCB-hard across training steps for 32B (left) and 7B (right) pure-reasoning runs. Shaded regions denote  $\pm 1$  standard deviation over three seeds.

**Failure-mode stability.** Figure 14 decomposes the failure rate on LCB-hard into *optimization failures* and *correctness failures*. The optimization-correctness trade-off reported in the main text is robust across seeds: stricter filtering ( $\text{Keep} \leq 10^3$ ) consistently yields higher optimization failure rates (32B:  $17.3 \pm 1.3\%$  vs.  $8.7 \pm 0.9\%$  for All tests at step 6k) while reducing correctness failure rates ( $37.5 \pm 0.7\%$  vs.  $49.0 \pm 3.3\%$ ). The same pattern holds at the 7B scale. In all cases the inter-seed standard deviation is substantially smaller than the inter-threshold differences, confirming that the reported trade-offs reflect genuine training dynamics rather than seed-dependent fluctuations.

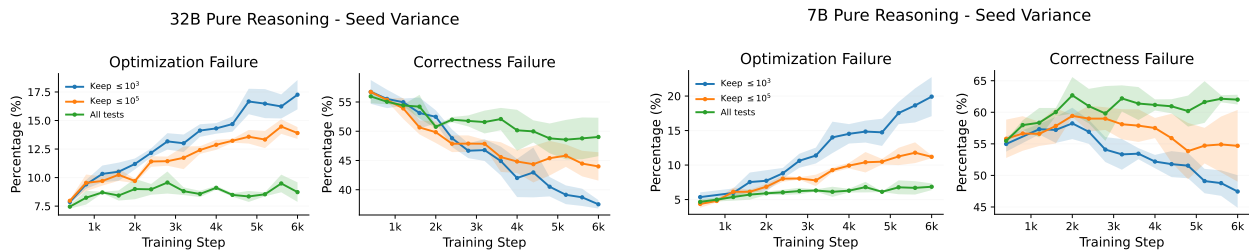


**Figure 14** Optimization failure and correctness failure rates on LCB-hard for 32B (left) and 7B (right). Shaded regions denote  $\pm 1$  standard deviation over three seeds. The trade-off between failure modes is consistent across seeds at both scales.

## C Experimental Details

### C.1 Test Input Length Distribution

Figure 15 compares the input character length distributions of CodeContests/train and CodeContestsPlus, alongside error decompositions of RL checkpoints trained on each and evaluated on LCB/hard. Despite having more test cases, CodeContests/train produces more optimization failures on LCB/hard (28.9% vs. 15.8%), because its tests rarely reach the input sizes that stress algorithmic efficiency. The number of tests alone does not determine coverage; it is the range of input sizes, and thus the optimization pressure they induce, that drives the trade-off frontier.

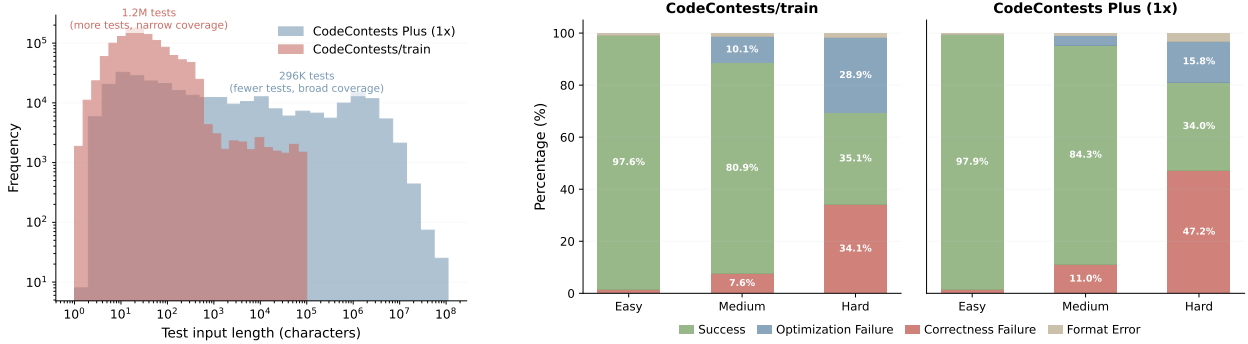


**Figure 15 Left:** Distribution of test case input lengths. CodeContestsPlus (blue) has fewer tests than CodeContests/train (red) but covers a much wider range of input sizes. **Right:** Error composition after RL training on CodeContests/train vs. CodeContestsPlus, by difficulty split on LCB. Despite having more tests, training on CodeContests/train produces more optimization failures on LCB/hard problems (28.9% vs. 15.8%), because its tests rarely reach the input sizes that stress algorithmic efficiency.

### C.2 7B Model SFT Training Details

We start from Qwen 2.5 7B (Qwen et al., 2025) base model and fine-tune on a mixture of OpenCodeReasoning-2 (Ahmad et al., 2025) (Python and C++) and OpenMathReasoning (Moshkov et al., 2025) for exactly 1 epoch. Training runs for 24,829 steps with 16 H100 nodes. We use the following hyperparameters: local batch size 2, sequence length 32,768, learning rate  $8.6 \times 10^{-6}$  with 1,000 warmup steps followed by a constant schedule, and gradient norm clipped at 1.0. We use FSDP in bf16 with tensor parallelism size 4. Linear layers use rowwise FP8 quantization (one scaling factor per matrix row for both activations and weights); all other computations are in bf16.

### C.3 7B Model RL Training Details

We train with a simplified asynchronous online RL recipe as shown in FAIR CodeGen team et al. (2025), namely Dr.GRPO (Liu et al., 2025) using DAPO-style (Yu et al., 2025) asymmetric clipping ( $\epsilon_{\text{low}}=0.2$ ,  $\epsilon_{\text{high}}=0.25$ ) and zero-advantage skipping, with no KL penalty ( $\beta=0$ ) and no reference model. Each prompt produces 16 rollouts at temperature 1.0. We use AdamW ( $\beta_1=0.9$ ,  $\beta_2=0.95$ , weight decay 0.1) with learning rate  $1.4 \times 10^{-7}$ , 100 warmup steps followed by a constant schedule, and gradient norm clipped at 0.1. Batching is token-based with a maximum of 32,768 tokens; sequence length is 32,768. The worker model is updated every 4 gradient steps in the trainer side. Training runs for 6,000 steps across 32 H100 nodes (no tensor parallelism) in bf16 with selective activation checkpointing, with 1:1 trainer:worker ratio. No FP8 is used for RL training.

We train on CodeContestsPlus (1x) with binary reward, sweeping the input-length threshold  $k \in \{2, \dots, 6, \infty\}$  across independent runs. Evaluation on LCB/v5 is with temperature 0.6, top- $p$  0.95, and 10 samples per problem. A single full RL run takes  $\sim 19$  hours wall-clock.

## C.4 32B Pure-Reasoning and Agentic Coding RL Training Details

Both the pure-reasoning and agentic-coding settings start from the same CWM-SFT 32B checkpoint and share most hyperparameters with the tool-use setting described above. We list the shared configuration first, then note setting-specific differences.

**Shared configuration.** Both settings use Dr.GRPO with DAPO-style asymmetric clipping ( $\epsilon_{\text{low}}=0.2$ ,  $\epsilon_{\text{high}}=0.25$ ) and zero-advantage skipping, with no KL penalty and no reference model. Reward function is binary. AdamW with learning rate  $1.4 \times 10^{-7}$ , constant schedule with 400-step warmup, and gradient norm clipped at 0.1. Each prompt produces 16 rollouts at temperature 1.0. The trainer-to-worker ratio is 1:1, with the model updated every 4 worker steps. Training uses 256 H100 GPUs (32 DP  $\times$  8 TP) with FSDP in bf16, torch.compile, and selective activation checkpointing. Pure reasoning trains for 8000 steps ( $\sim 44$  hours per run); agentic coding trains for 4000 steps ( $\sim 16$  hours per run). We sweep the input-length threshold  $k \in \{2, \dots, 6, \infty\}$  across independent runs, identical to the tool-use setting.

**Pure reasoning.** The pure-reasoning setting use sequence length 32768 and no tool calls. The model generates a single reasoning trace in a `<think>` block followed by the code submission. Evaluation uses temperature 0.6 and top- $p$  0.95 with 10 samples per problem.

**Agentic coding.** The agentic setting uses a sandboxed terminal environment backed by Modal, a cloud sandbox service, with sequence length 61440 and up to 72 interaction turns per trajectory. The model can execute arbitrary shell commands, write and run code, and observe terminal output within a sandbox that enforces a 120-second session timeout and 1-8 GB memory limits with network access blocked. Evaluation uses temperature 1.0 and top- $p$  0.95 with 5 samples per problem.

## C.5 32B Tool-Use Model Training Details

We describe two parts of the 32B tool-use setup here.

First, two RL-to-SFT bootstrapping iterations build one shared SFT initialization, because CWM-SFT does not reliably use our stdin-oriented `python-io` interface for competitive-programming tasks.

Second, starting from that same initialization, i.e., SFT checkpoint, the final RL phase launches the verifier-strictness sweep analyzed in the main text. In this final sweep, the compared checkpoints are trained under nested binary coverage rewards, with the task distribution, tool interface, and RL hyperparameters fixed across thresholds. Thus the comparison varies unit-test coverage, not the earlier bootstrapping curriculum.

The bootstrapping iteration proceeds as follows:

1. **Iteration 0 (RL).** Starting from CWM-SFT, run RL with reward shaping on competitive-programming problems to teach the model to invoke a Python interpreter that accepts standard input (`python-io`). Correct trajectories are collected, filtered and downsampled for SFT.
2. **Iteration 1 (SFT  $\rightarrow$  RL).** Distill the collected tool-use trajectories from Iteration 0 via SFT back into CWM-SFT; then run RL on CodeContestsPlus with reward shaping that encourages a stress-testing tool (`python-stress`), lets the model generate large inputs and check whether its solution timeouts. This tool functions the same as normal python tool but uses a different name for better behavior tracking. Correct trajectories are collected, filtered and downsampled for SFT.
3. **Iteration 2 (SFT).** Distill the collected tool-use trajectories from Iteration 1 via SFT back into CWM-SFT.

Finally, we launch the RL sweep under different input thresholds, starting with the SFT checkpoint produced from Iteration 2.

### C.5.1 Iteration 0: Tool-Use RL

We start from CWM-SFT 32B, which can reason in a `<think>` block but has never used a Python tool for code that reads from stdin. We run RL with Dr.GRPO on CodeContests/train (12275 problems) with two tools available: `python` (execute a code snippet) and `python-io` (execute code that requires stdin). The

prompt includes a small number of few-shot examples demonstrating `python-io` usage. The reward function gives hierarchical partial credit for tool invocation: full reward (+1) for passing with `python-io` in the first turn, reduced credit (+0.8, +0.5, 0) for passing with progressively less desirable tool usage, and asymmetric penalties on failure that are smaller when the model at least attempted tool use. This encourages the model to explore tool use early in training.

### C.5.2 Iteration 1: Distillation and Stress-Testing RL (SFT $\rightarrow$ RL)

**SFT phase.** From the Iteration 0 RL run, we collect trajectories that (i) contain at least one `python-io` call and (ii) lead to a correct final answer. We apply diversity filtering to balance across dialog lengths, tool usage patterns, and task coverage, reducing the dataset from 804k to 276k examples. We also filter to a maximum of 32 768 tokens per trajectory and reformat reasoning tokens from the `<think>` tag into the native `<|reasoning_thinking_start|>` format reserved for CWM-SFT. SFT trains for 1 600 steps at learning rate  $10^{-6}$ , starting again from CWM-SFT but not the RL checkpoint, with batch size 2 and sequence length 32 768 across 32 H100 nodes (32 DP  $\times$  8 TP). Linear layers use rowwise FP8 quantization; all other computations are in bf16.

**RL phase.** Starting from the SFT checkpoint, we run RL on CodeContestsPlus (1 $\times$ ) with the same tool-use environment as iteration 0 plus the `python-stress` tool, which lets the model write an input generator alongside its solution and reports wall-clock execution time. The reward function shifts the shaping target from `python-io` to `python-stress`: full reward (+1) for passing when `python-stress` was used anywhere in the trajectory, reduced credit (+0.5) for passing with only generic tool use, and a small penalty ( $-0.2$ ) for failing despite using `python-stress` versus full penalty ( $-1$ ) for failing without any tool use. This encourages the model to adopt stress testing for efficiency verification before submission.

## C.6 Iteration 2: Distillation and RL Sweep

**SFT phase.** We adopt the same SFT strategy as Iteration 1. Instead of merge the SFT dataset gathered from Iteration 0 and Iteration 1, we use exclusively the dataset from Iteration 1 which supersedes the behavior presented in Iteration 0. We use the same hyperparameters and training steps as in Iteration 1.

**RL phase.** Starting from the SFT checkpoint, we run RL on CodeContestsPlus (1 $\times$ ) with the same tool-use environment as iteration 1. The reward function becomes binary which grades only the final correctness. This is the RL run where we sweep different test coverage threshold.

### C.6.1 Shared RL hyperparameters

Both RL iterations use Dr.GRPO (Liu et al., 2025) with DAPO-style (Yu et al., 2025) asymmetric clipping ( $\epsilon_{\text{low}}=0.2$ ,  $\epsilon_{\text{high}}=0.25$ ) and zero-advantage skipping, with no KL penalty and no reference model. We use AdamW with learning rate  $1.4 \times 10^{-7}$ , constant schedule with 400-step warmup, and gradient norm clipped at 0.1. Each prompt produces 16 rollouts at temperature 1.0, with a maximum of 6 tool calls per trajectory. The trainer-to-worker ratio is 1:1, with the model updated every 4 worker steps. Training uses 256 H100 GPUs (32 DP  $\times$  8 TP) with FSDP in bf16, torch.compile, and selective activation checkpointing. The two iterations differ in training data, reward target, sequence length, and step count: iteration 0 trains for 4 000 steps on CodeContests/train with `python-io` reward shaping and sequence length 131 072; iteration 1 and 2 trains for 8 000 steps on CodeContestsPlus (1 $\times$ ) with `python-stress` reward shaping and binary pass-fail reward respectively and sequence length 65 536 (approximately 18 hours per run).

**Observation.** During iteration 0, we ran RL on both DMC/train and CodeContestsPlus. The two training sets yield similar overall pass rates, but different error profiles: CodeContestsPlus produces fewer timeouts and more wrong answers. This observation motivated the core investigation of this paper (Section 3).

### C.6.2 Example trajectories

We show one representative trajectory from each iteration to illustrate the tool-use patterns the model acquires. Thinking blocks are truncated for space; all code and tool output are shown verbatim.

**Iteration 0: testing with python-io.** The system prompt gives the model access to `python` and `python-io` tools with a budget of 5 tool turns. The following trajectory solves a phone-keypad cipher problem.

### System Prompt (Iteration 0)

You are an expert Python programmer and tool user. You have access to "python" and "python-io" tools. You are constrained by a 61440 total context window limit. You can interact with these tools through the following tool interface for at most 5 turns.

```
<tool: python>
Run Python code in an isolated sandbox.
</tool>
```

```
<tool: python-io>
Run Python code with stdin input in an isolated sandbox.
Use <code>...</code> for code and <stdin>...</stdin> for input.
</tool>
```

You will receive a budget notice after each tool execution indicating your remaining turns and tokens.

### User

Provide a Python solution for the following competitive programming question: Solve The Mystery

Input:

First line contains T - number of test cases.  
Following T lines each contains a string of characters in [a-z] only

Output: Print a numeric string for each test case.

Constraints:  $1 \leq T \leq 100$ ,  $1 \leq \text{Length of String} \leq 100$

SAMPLE INPUT	SAMPLE OUTPUT
10	539
key	86
to	2668765
control	6463
nine	82457
tails	47
is	46
in	9687
your	4263
hand	74663
phone	

### Assistant – Turn 1 (python-io)

```
<think>
I need to map each letter to its phone keypad digit. Looking at the
sample: k->5, e->3, y->9 gives "539". This is the standard phone
keypad mapping: abc->2, def->3, ghi->4, jkl->5, mno->6, pqrs->7,
tuv->8, wxyz->9.
</think>
```

```
<tool: python-io>
<code>
keypad = {
    'a': '2', 'b': '2', 'c': '2',
    'd': '3', 'e': '3', 'f': '3',
    'g': '4', 'h': '4', 'i': '4',
    'j': '5', 'k': '5', 'l': '5',
    'm': '6', 'n': '6', 'o': '6',
    'p': '7', 'q': '7', 'r': '7', 's': '7',
    't': '8', 'u': '8', 'v': '8',
    'w': '9', 'x': '9', 'y': '9', 'z': '9'
}
t = int(input())
for _ in range(t):
    s = input().strip()
    print(''.join(keypad[c] for c in s))
</code>
<stdin>
10
```

```
key
to
control
nine
tails
is
in
your
hand
phone
</stdin>
</tool>
```

### Tool Response

```
completed. [stdout]539
86
2668765
6463
82457
47
46
9687
4263
74663[/stdout]

<budget> Remaining turns: 4, Remaining tokens: 59534 </budget>
```

### Assistant – Turn 2 (python-io): Edge cases

```
<think>
The sample output matches. Let me test edge cases: 4-letter groups
(pqrs, wxyz), single characters, and all-same-group strings.
</think>

<tool: python-io>
<code>
keypad = { ... } # same dictionary as above
t = int(input())
for _ in range(t):
    s = input().strip()
    print(''.join(keypad[c] for c in s))
</code>
<stdin>
5
aaa
pqrs
wxyz
a
z
</stdin>
</tool>
```

### Tool Response

```
completed. [stdout]222
7777
9999
2
9[/stdout]

<budget> Remaining turns: 3, Remaining tokens: 59081 </budget>
```

### Assistant – Final Submission

```
<think>
All edge cases pass. The solution handles all constraints correctly.
</think>

```python
keypad = {
    'a': '2', 'b': '2', 'c': '2',
    'd': '3', 'e': '3', 'f': '3',
```

```

    'g': '4', 'h': '4', 'i': '4',
    'j': '5', 'k': '5', 'l': '5',
    'm': '6', 'n': '6', 'o': '6',
    'p': '7', 'q': '7', 'r': '7', 's': '7',
    't': '8', 'u': '8', 'v': '8',
    'w': '9', 'x': '9', 'y': '9', 'z': '9'
}
t = int(input())
for _ in range(t):
    s = input().strip()
    ... print(''.join(keypad[c] for c in s))
...

```

**Iteration 1: stress-testing with python-stress.** The system prompt adds the `python-stress` tool, which runs code with automatic timing and memory measurement. The following trajectory solves a prefix-sum divisibility counting problem ( $N \leq 10^5$ , time limit 2s).

### System Prompt additions (Iteration 1)

You have access to "python", "python-io" and "python-stress" tools.

<tool: python-stress>

Run Python code with performance testing and automatic output suppression to save context. This tool automatically measures execution time and memory usage.

IMPORTANT: Output is limited to the last 50 lines. Use this for efficiency testing with large inputs. You MUST generate test cases programmatically inside the code - do not use <stdin>.

DO NOT print large data structures - only print performance metrics.

</tool>

### User

Provide a Python solution for the following competitive programming question. Time Limit: 2.0 s. Memory Limit: 1073 MB.

There are  $N$  boxes arranged in a row from left to right. The  $i$ -th box from the left contains  $A_i$  candies. You will take out the candies from some consecutive boxes and distribute them evenly to  $M$  children.

Find the number of pairs  $(l, r)$  such that  $1 \leq l \leq r \leq N$  and  $A_l + A_{l+1} + \dots + A_r$  is a multiple of  $M$ .

Constraints:  $1 \leq N \leq 10^5$ ,  $2 \leq M \leq 10^9$ ,  $1 \leq A_i \leq 10^9$

Examples:

```

3 2 / 4 1 5          -> 3
13 17 / 29 7 ... 81 -> 6
10 400000000 / 10^9 x10 -> 25

```

### Assistant – Turn 1 (python-io): Parse input

<think>

This is a classic prefix-sum modulo problem. First let me validate the input parsing.

</think>

<tool: python-io>

<code>

```

n, m = map(int, input().split())
a = list(map(int, input().split()))
print(f"N: {n}, M: {m}, Array: {a}")

```

</code>

<stdin>

```

3 2
4 1 5

```

</stdin>

</tool>

### Tool Response

```
completed. [stdout]N: 3, M: 2, Array: [4, 1, 5][/stdout]
<budget> Remaining turns: 4, Remaining tokens: 61155 </budget>
```

### Assistant – Turn 2 (python): Core algorithm test

```
<think>
Now test the prefix-sum-modulo + frequency-counting approach.
</think>

<tool: python>
def solve():
    n, m = 3, 2
    a = [4, 1, 5]
    count = 0
    mod_freq = {0: 1}
    prefix_sum_mod = 0
    for num in a:
        prefix_sum_mod = (prefix_sum_mod + num) % m
        if prefix_sum_mod in mod_freq:
            count += mod_freq[prefix_sum_mod]
            mod_freq[prefix_sum_mod] = mod_freq.get(
                prefix_sum_mod, 0) + 1
    print(f"Count: {count}")
    assert count == 3
solve()
</tool>
```

### Tool Response

```
completed. [stdout]Count: 3[/stdout]
<budget> Remaining turns: 3, Remaining tokens: 60885 </budget>
```

### Assistant – Turn 3 (python-io): Full solution test

```
<think>
Core logic works. Now test the full solution with stdin.
</think>

<tool: python-io>
<code>
def solve():
    n, m = map(int, input().split())
    a = list(map(int, input().split()))
    count = 0
    mod_freq = {0: 1}
    prefix_sum_mod = 0
    for num in a:
        prefix_sum_mod = (prefix_sum_mod + num) % m
        if prefix_sum_mod in mod_freq:
            count += mod_freq[prefix_sum_mod]
            mod_freq[prefix_sum_mod] = mod_freq.get(
                prefix_sum_mod, 0) + 1
    print(count)
solve()
</code>
<stdin>
3 2
4 1 5
</stdin>
</tool>
```

### Tool Response

```
completed. [stdout]3[/stdout]
<budget> Remaining turns: 2, Remaining tokens: 60663 </budget>
```

### Assistant – Turn 4 (python-stress): Performance test

```
<think>
Solution is correct. Now stress-test at scale to confirm  $O(n)$ 
performance within the 2s time limit.
</think>

<tool: python-stress>
import random, time

def solve(n, m, arr):
    count = 0
    mod_freq = {0: 1}
    prefix_sum_mod = 0
    for num in arr:
        prefix_sum_mod = (prefix_sum_mod + num) % m
        if prefix_sum_mod in mod_freq:
            count += mod_freq[prefix_sum_mod]
            mod_freq[prefix_sum_mod] = mod_freq.get(
                prefix_sum_mod, 0) + 1
    return count

print("PERFORMANCE PROFILE")
print("=" * 60)
for size in [10**3, 10**4, 10**5]:
    arr = [random.randint(1, 10**9) for _ in range(size)]
    start = time.time()
    solve(size, 10**9, arr)
    elapsed = time.time() - start
    print(f"n={size:>8} Time: elapsed:>6.3fs PASS")
print("=" * 60)
</tool>
```

### Tool Response

```
completed. [stdout]PERFORMANCE PROFILE
=====
n=   1000 Time: 0.000s PASS
n=  10000 Time: 0.004s PASS
n= 100000 Time: 0.048s PASS
=====[/stdout]
[performance] Execution Time: 0.277s, Peak Memory: 25.3 MB
<budget> Remaining turns: 1, Remaining tokens: 60169 </budget>
```

### Assistant – Final Submission

```
<think>
Solution passes all tests and runs well within the 2s time limit
at  $n=10^5$ . Submit with sys.stdin.read() optimization.
</think>

```python
def solve():
    import sys
    input = sys.stdin.read
    data = input().split()
    n = int(data[0])
    m = int(data[1])
    a = list(map(int, data[2:2+n]))
    count = 0
    mod_freq = {0: 1}
    prefix_sum_mod = 0
    for num in a:
        prefix_sum_mod = (prefix_sum_mod + num) % m
        if prefix_sum_mod in mod_freq:
            count += mod_freq[prefix_sum_mod]
            mod_freq[prefix_sum_mod] = mod_freq.get(
                prefix_sum_mod, 0) + 1
    print(count)
solve()
```
```

## C.7 Compute Resources

All experiments use NVIDIA H100 80 GB GPUs. Table 1 summarizes the hardware layout and wall-clock time for each training configuration. For the 7B, 32B pure-reasoning, and 32B agentic-coding settings, we sweep the input-length threshold  $k \in \{2, \dots, 6, \infty\}$  across six independent runs; total GPU-hours for those rows reflect this  $\times 6$  factor. The 32B tool-call pipeline requires a bootstrapping phase (2 RL + 2 SFT runs) before the final threshold sweep. The bootstrapping rows are single runs. The Iter 0 RL uses 131k sequence length while the Iter 1 RL uses 64k sequence length, which compensates the training steps and results in roughly the same wall-clock training time.

**Table 1** Compute resources per training configuration. DP = data parallelism, TP = tensor parallelism. Bootstrapping rows (marked †) are single runs that build the starting policy for the tool-call threshold sweep.

| Setting                                                      | Model | GPUs | DP $\times$ TP | Steps | Hours/run | Total GPU-h    |
|--------------------------------------------------------------|-------|------|----------------|-------|-----------|----------------|
| <i>Threshold-swept settings (<math>\times 6</math> runs)</i> |       |      |                |       |           |                |
| 7B pure reasoning RL                                         | 7B    | 32   | 32 $\times$ 1  | 6 000 | $\sim 19$ | $\sim 3\,648$  |
| 32B pure reasoning RL                                        | 32B   | 256  | 32 $\times$ 8  | 8 000 | $\sim 44$ | $\sim 67\,584$ |
| 32B tool-call RL                                             | 32B   | 256  | 32 $\times$ 8  | 8 000 | $\sim 18$ | $\sim 27\,648$ |
| 32B agentic coding RL                                        | 32B   | 256  | 32 $\times$ 8  | 4 000 | $\sim 16$ | $\sim 24\,576$ |
| <i>Tool-call bootstrapping† (2 RL + 2 SFT, single runs)</i>  |       |      |                |       |           |                |
| Iter 0 RL                                                    | 32B   | 256  | 32 $\times$ 8  | 4 000 | $\sim 18$ | $\sim 4\,608$  |
| Iter 1 SFT                                                   | 32B   | 256  | 32 $\times$ 8  | 1 600 | $< 1$     | $\sim 256$     |
| Iter 1 RL                                                    | 32B   | 256  | 32 $\times$ 8  | 8 000 | $\sim 18$ | $\sim 4\,608$  |
| Iter 2 SFT                                                   | 32B   | 256  | 32 $\times$ 8  | 1 600 | $< 1$     | $\sim 256$     |

## D Extended Frontier Evidence

### D.1 Per-setting extrapolation plots

Figures 1 and 5 in the main text show the extrapolative continuation as compact panels. This subsection presents standalone plots for each setting and scale with full interpolation, extrapolation, and format-error detail.

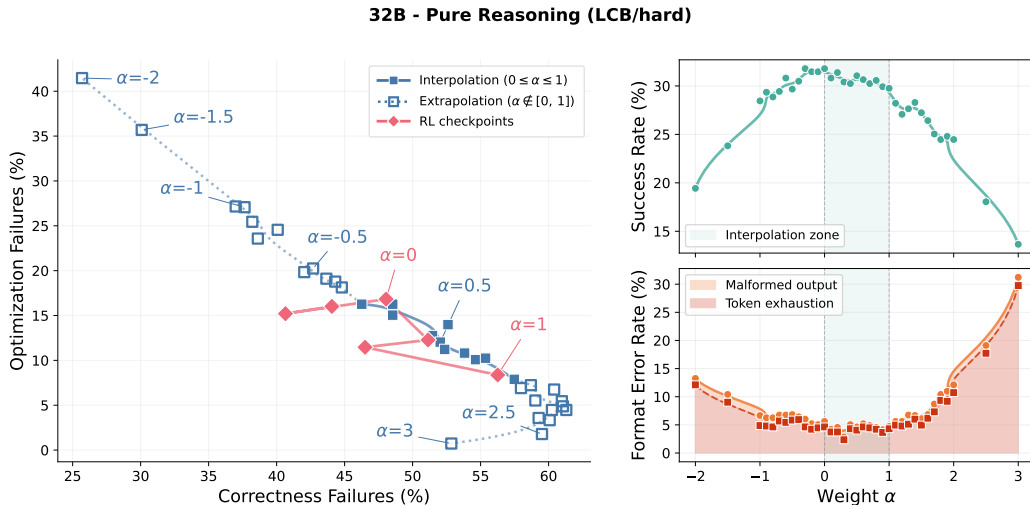


**Figure 16** 32B pure reasoning on LCB/hard.

### 32B - Agentic Coding (LCB/hard)

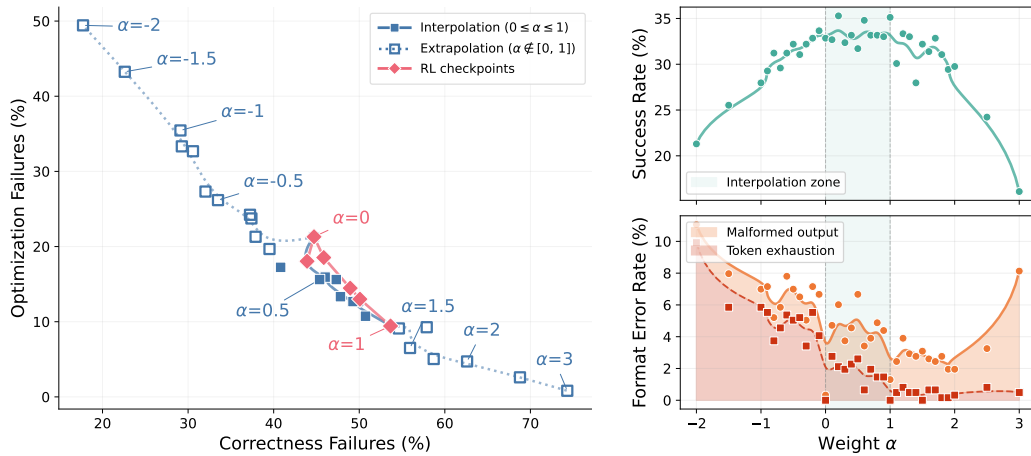


Figure 17 32B agentic coding on LCB/hard.

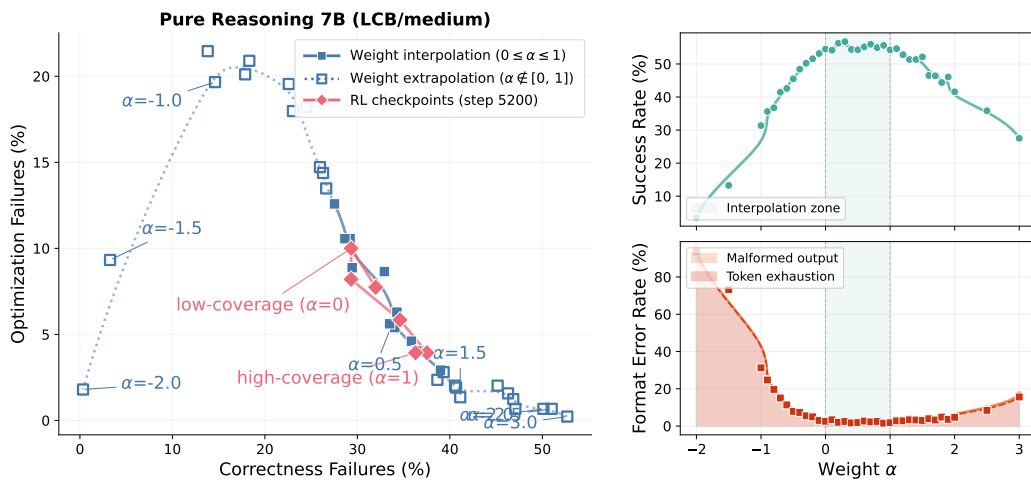


Figure 18 7B pure reasoning on LCB/medium (capability-matched split).

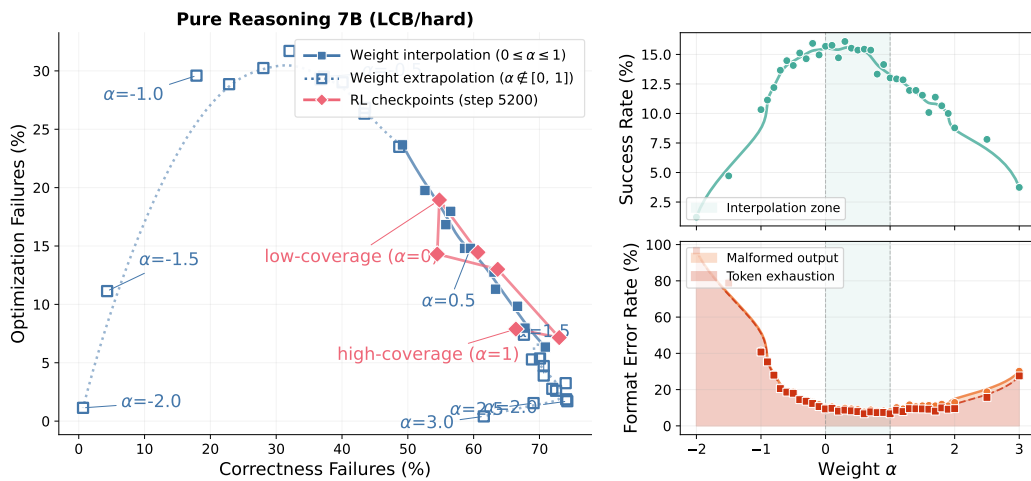
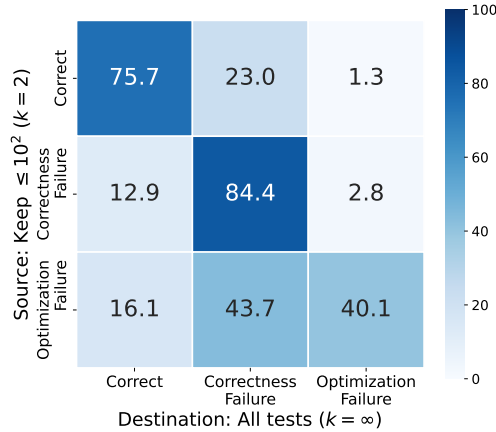


Figure 19 7B pure reasoning on LCB/hard. The stable extrapolation range is narrower than LCB/medium, with format errors dominating earlier on the low- $\alpha$  side.

## D.2 Full Pairwise Transition Matrices



**Figure 20** Task-level transition matrix from  $k=2$  ( $\text{keep} \leq 10^2$ ) to  $k=\infty$  (all tests) on 123 hard problems. Taken from pure-reasoning setting in late stage of the training (7.2k steps). Rows are normalized to 100%. Of optimization failures under low coverage, 43.7% become correctness failures under high coverage, ruling out an aggregation artifact.

Figure 21 shows the complete set of task-level transition matrices between all pairs of test-coverage conditions on hard problems. The pattern is consistent throughout: the dominant off-diagonal transitions are between optimization failures and correctness failures, confirming that the trade-off operates at the individual task level across all condition pairs.

## D.3 Emergence of the Trade-off Curve During Training

The trade-off curve emerges progressively during RL training. At step 400 (Figure 22, left), all six conditions cluster in a tight region of the (Correctness Failure, Optimization Failure) plane. By step 3600 (center), the runs have diverged along a clear trade-off curve, with the ordering matching the test-coverage threshold monotonically. By step 6400 (right), the separation widens further. This divergence occurs relatively early in training and then stabilizes, suggesting that RL quickly discovers the point on the frontier dictated by its test-coverage level.

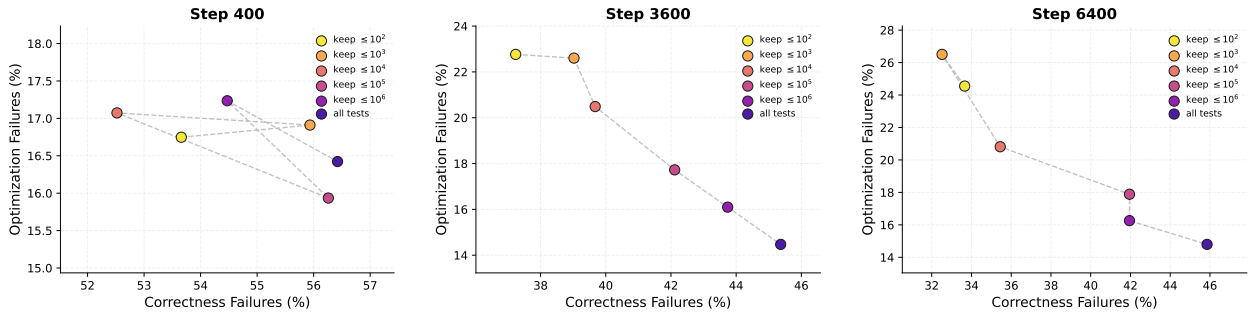


**Figure 22** Emergence of the trade-off curve during RL training. At step 400, all six test-coverage conditions are clustered together. By step 3600, they have spread into a clear trade-off curve. By step 6400, the separation widens further.

## D.4 Training Dynamics

Figure 23 shows the optimization-failure and correctness-failure counts over an extended training horizon on 32B pure-reasoning setting. The separation between conditions is sustained at later steps, indicating that the trade-off is not a transient phenomenon of early training.

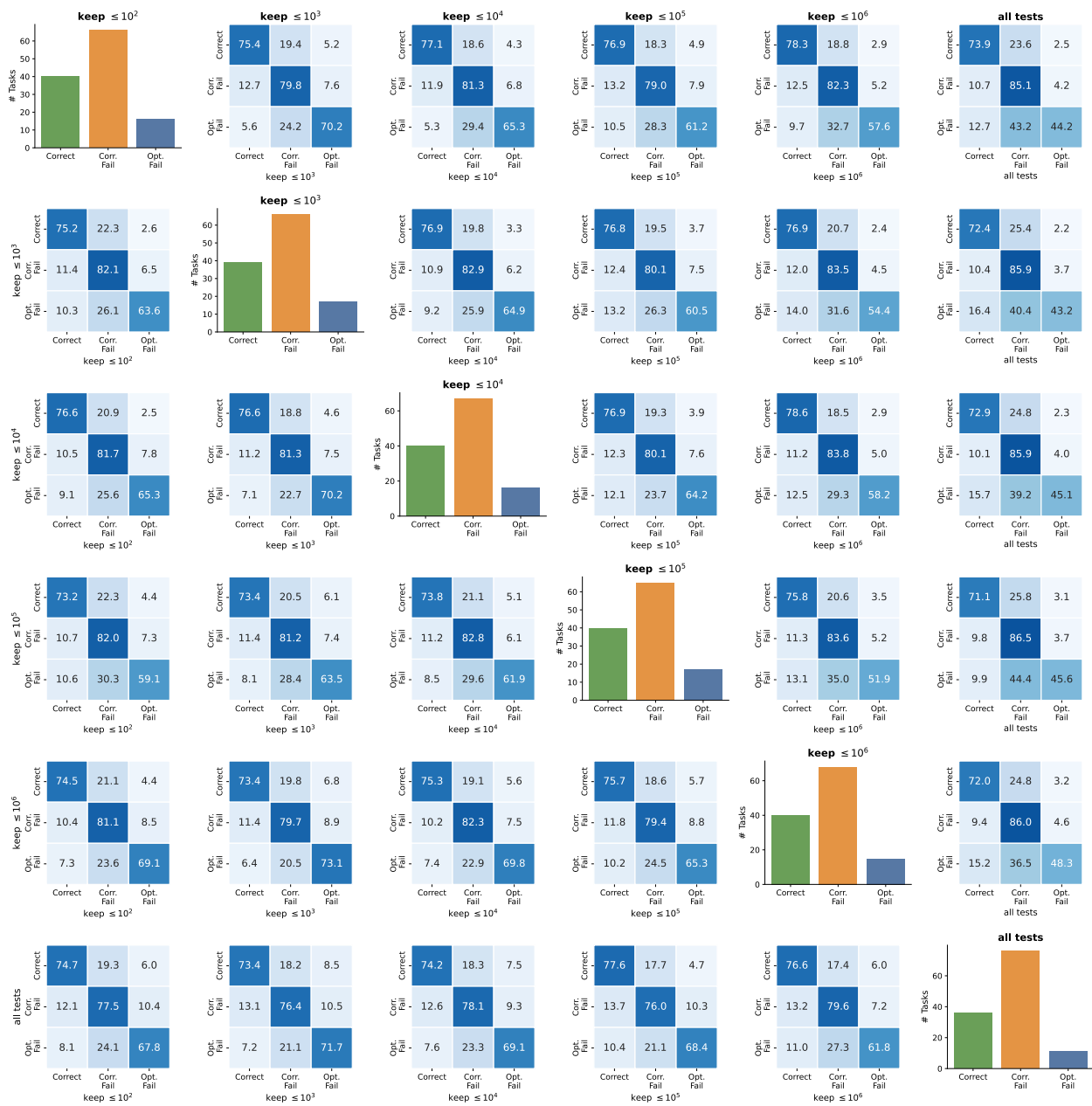


**Figure 21** Full grid of pairwise task-level transition matrices on hard problems. Diagonal panels show per-condition status distributions. Taken from the pure-reasoning setting in early stage of the training (3.6k steps). Off-diagonal cells are row-normalized to 100%.

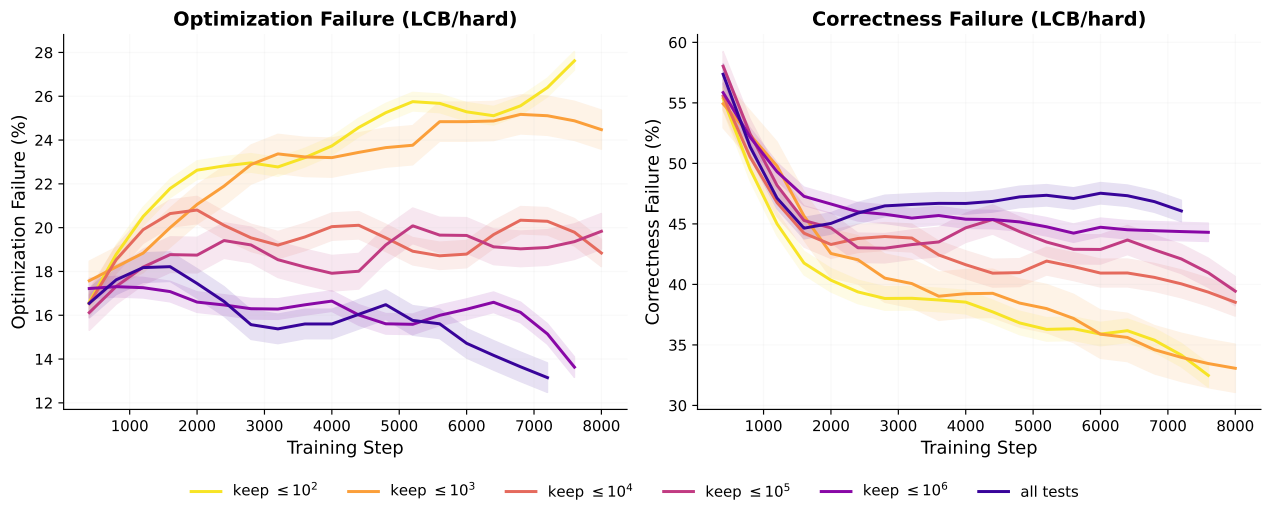


**Figure 23** Extended training dynamics showing optimization-failure and correctness-failure counts on hard problems vs. training step on LCB/hard.

## E Inference-Time Ensemble Details

### E.1 Full Solved-Set Overlap

Section 4.1 reports overlap numbers within the interpolation range. Figure 24 extends this to the full extrapolation range  $\alpha \in [-2, 3]$ . The gradual-drift pattern persists: overlap decreases monotonically with distance in  $\alpha$ . Even at the extremes ( $\alpha = -2$  vs.  $\alpha = 3$ ), the Jaccard similarity remains above 0.54, indicating that over half of solved problems are shared. The matrix is approximately symmetric about the diagonal, consistent with a smooth, one-dimensional manifold of solved sets.

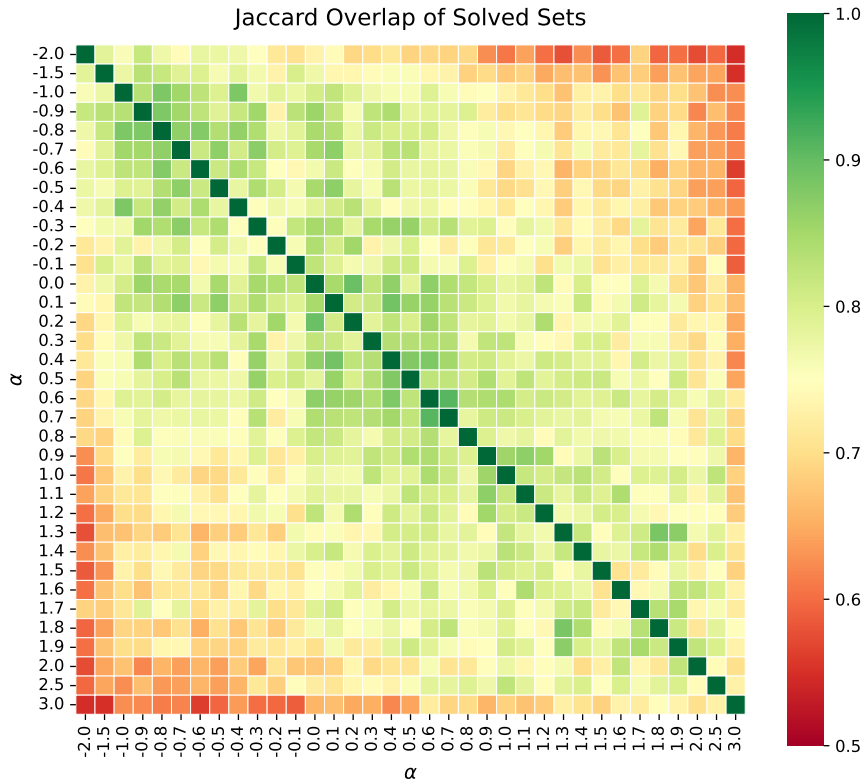


**Figure 24** Full pairwise Jaccard similarity between solved sets across the extrapolation range  $\alpha \in [-2, 3]$ . Overlap decreases steadily with distance in  $\alpha$  but remains above 0.54 even at the extremes, confirming gradual drift of the success set across the entire interpolation and extrapolation range.

### E.2 Coverage headroom decomposition

Different checkpoints along the interpolation axis solve different subsets of hard problems, so pooling multiple checkpoints and selecting the best submission per problem can exceed the solve rate of every individual checkpoint. We quantify this *coverage headroom* with a greedy set-cover procedure: at each step, the checkpoint whose solved set adds the most new problems is appended to the pool, and we track the cumulative number of problems solved by at least one member. Figure 25 (left) shows the resulting curve for interpolation-only and interpolation-plus-extrapolation pools; the right panel decomposes the total gain over the best single checkpoint into contributions from each regime.

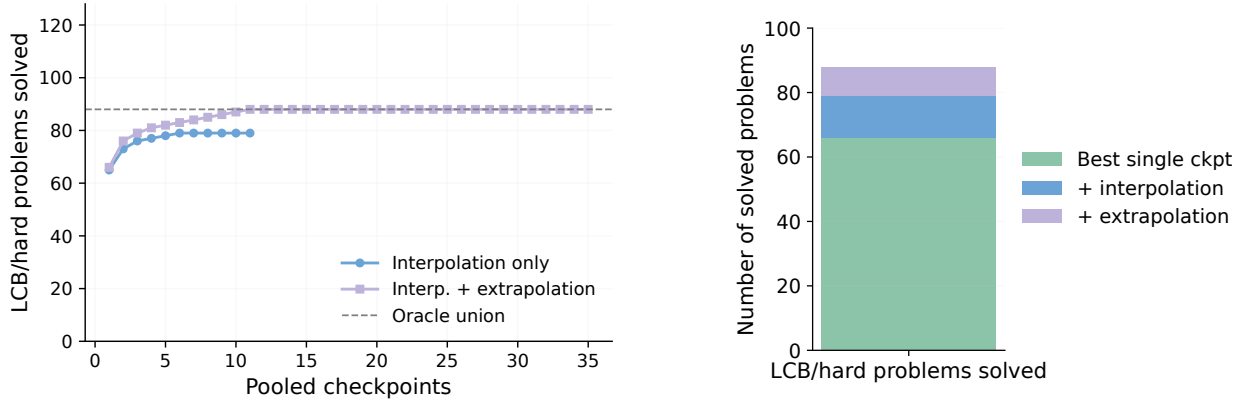


**Figure 25 Left:** Cumulative coverage of LCB/hard (123 problems) as a function of the number of checkpoints in the pool, under a greedy ordering. The interpolation-only pool (blue) plateaus at 79 problems; admitting extrapolated checkpoints (red) continues to grow until it reaches 88. **Right:** Decomposition of the 22-problem coverage gain over the best single checkpoint into the contributions from interpolation and extrapolation. Extrapolation accounts for 9 of the 22 extra problems and is the only path to the final coverage band.

### E.3 Filtered submission budgets on LCB/v5

In practice, competitive programming judges allow only a handful of submissions per problem, so raw  $\text{pass}@k$  with large  $k$  overstates the value of a diverse candidate pool.  $\text{Pass } n@k$  measures the solve rate when  $k$  candidates are sampled, filtered by public tests, and the top  $n$  are submitted. Figure 26 fixes  $k=250$  and sweeps  $n$  from 1 to 250 on the LCB/v5 hard split. The extrapolation-inclusive five-checkpoint pool dominates the best single RL checkpoint and the interpolation-only pool at every submission budget. At  $n=1$ , also called  $\text{best}@k$ , the gap is already roughly two percentage points, showing that even a single filtered submission benefits from the broader coverage of the extrapolated checkpoints. The per-problem oracle selects the best checkpoint for each problem independently; the extrapolation pool nearly closes this gap by  $n=250$ .

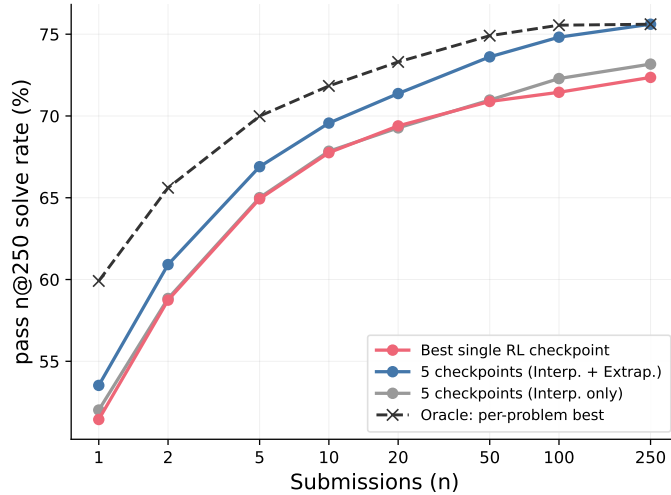


**Figure 26** Pass  $n@250$  with public-test filtering on LCB/v5 hard. The extrapolation-inclusive five-checkpoint pool is higher than both the best single checkpoint and the interpolation-only pool at each displayed submission budget  $n$ . This is an in-domain diagnostic of how filtering converts candidate diversity into gains under smaller submission budgets.

## F Reward Shaping Experiments

Reward shaping is the simplest static attempt to soften the binary pass-fail reward. It assigns partial credit for progress on the same test suite, but it never reveals why a rollout failed. It therefore changes the scalarization of the same nested test outcomes without changing the information available to learning. The definitions below make this limitation concrete.

In the reward-shaping experiment, the model receives partial credit according to the largest test-coverage threshold its submission passes. We use the threshold set  $\mathcal{K} = \{2, 3, 4, 5, 6, \infty\}$ . The shaped reward is

$$R_{\text{shape}}(y) = \begin{cases} 0 & \text{fails some test with input length } \leq 10^2, \\ 1/6 & \text{passes all tests with input length } \leq 10^2, \\ 2/6 & \text{passes all tests with input length } \leq 10^3, \\ 3/6 & \text{passes all tests with input length } \leq 10^4, \\ 4/6 & \text{passes all tests with input length } \leq 10^5, \\ 5/6 & \text{passes all tests with input length } \leq 10^6, \\ 1 & \text{passes all tests.} \end{cases} \quad (3)$$

Because the thresholded rewards are nested, this partial-credit objective is exactly the average of the binary rewards from Section 2:

$$R_{\text{shape}}(y) = \frac{1}{|\mathcal{K}|} \sum_{k \in \mathcal{K}} R_k(y). \quad (4)$$

This identity is the main reason reward shaping behaves like a reweighting of the same static outcome family rather than a new source of information.

**Why shaping stays on the frontier: a KL-regularized lens.** Our actual training uses Dr.GRPO without an explicit KL penalty. To build intuition for why reward shaping does not escape the frontier, we analyze a simplified KL-regularized surrogate. The argument is not a claim about GRPO dynamics; it is a closed-form calculation that illustrates why static shaping recombines existing outcome information rather than introducing new signal.

For a reward  $R$  and reference policy  $\pi_0$ , it is known that the KL-regularized optimal policy with KL penalty  $\beta$  is

$$\pi^*(y | x) \propto \pi_0(y | x) \exp(R(y)/\beta). \quad (5)$$

Write  $\pi_k^*$  for the optimum under the single-threshold binary reward  $R_k$ . Substituting  $R_{\text{shape}} = \frac{1}{|\mathcal{K}|} \sum_k R_k$  gives

$$\begin{aligned} \pi_{\text{shape}}^*(y | x) &\propto \pi_0(y | x) \exp\left(\frac{1}{|\mathcal{K}|\beta} \sum_{k \in \mathcal{K}} R_k(y)\right) \\ &\propto \left(\prod_{k \in \mathcal{K}} \pi_k^*(y | x)\right)^{1/|\mathcal{K}|}. \end{aligned} \quad (6)$$

The optimal policy for the shaped reward is therefore the normalized geometric mean of the single-threshold optimal policy, or equivalently the softmax of their arithmetic-mean logits. Because  $\pi_{\text{shape}}^*$  is fully determined by the single-threshold optima  $\{\pi_k^*\}$ , reward shaping recombines the same nested outcome information rather than introducing a genuinely new training signal. This provides intuition for why shaped rewards do not escape the frontier in our experiments, although we note that the geometric mean is not a convex combination in the probability simplex, so a formal convex-hull guarantee does not follow from this analysis alone.

This echoes the geometry of Section 3: weight averaging combines the same family of policies in parameter space, and reward shaping combines them in reward space. These two can be connected if the model weights are under small perturbation that can be linearly approximated.

**Continuous reward shaping.** In addition to the discrete variant above, we test a continuous variant that interpolates linearly in log-space based on the smallest failing test input. Let  $s(y)$  denote the character length of the smallest test input on which submission  $y$  fails. The continuous shaped reward is

$$R_{\text{cont}}(y) = \begin{cases} 1 & \text{passes all tests,} \\ \frac{\log_{10} s(y) - 2}{4} & 10^2 \leq s(y) < 10^6, \\ 0 & s(y) < 10^2. \end{cases} \quad (7)$$

This interpolates linearly in log-space from 0 (fails on the smallest inputs) to 1 (passes everything). Both variants remain static functions of the same test outcomes. As Figure 28 shows, both land on the existing trade-off curve, with continuous reward shaping slightly worse. We posit that the scalarization does not matter and what matters is that neither variant reveals why a submission failed.

Figure 27 shows the training dynamics for the two shaped-reward runs.

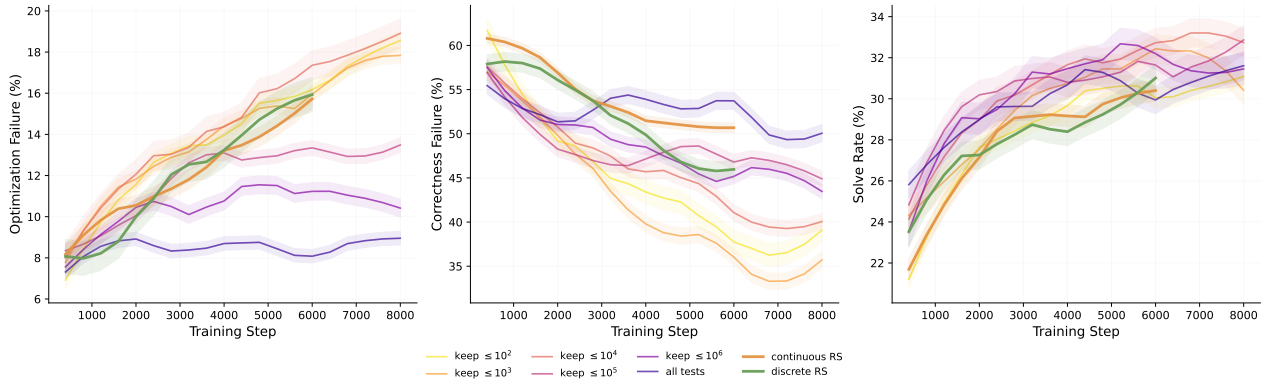


**Figure 27** Training dynamics of 32B pure-reasoning setting under reward shaping. Partial credit produces a smoother reward signal but does not improve the final solve rate. The shaped-reward policy converges to the same region of the trade-off curve as the corresponding uniform-weight binary-reward baseline.

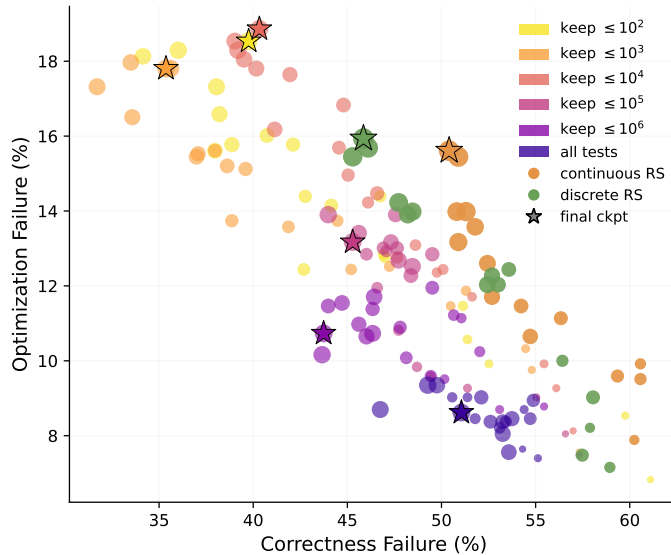


**Figure 28** Reward shaping lands on the existing trade-off curve (32B pure reasoning, LCB/hard). Larger dots stand for later stage of training. Baseline single-threshold runs are shown as a color gradient from low coverage to high coverage. Both discrete (green) and continuous (orange) reward shaping checkpoints fall on the same frontier. Stars mark final checkpoints. Reward shaping, whether discrete or continuous, cannot escape the trade-off.

## G Failure-Conditioned Training Experiments

### G.1 Repair Prompt and Repairability Metric

The repair prompt  $z = \phi(x, y)$  concatenates the original problem statement  $x$ , the failed code  $y$ , and aggregated execution statistics, along with brief advice on interpreting each failure type. It does not expose private test inputs, expected outputs, or detailed failing traces.

We define  $\text{fix}@k$  as the  $\text{pass}@k$  of repair attempts conditioned on a failed original sample. Similar to  $\text{pass}@k$ , we report the aggregate number across all the fixing prompts created from the failing attempts.

### G.2 Online-Fixing Objective

For a prompt  $x \sim \mathcal{D}$ , let  $y \sim \pi_\theta(\cdot | x)$  be a rollout and  $z = \phi(x, y)$  the fixing prompt constructed from  $x$  and its failed code  $y$ . The online-fix objective adds a failure-conditioned correction term to the standard GRPO loss  $\mathcal{L}_{\text{GRPO}}$ :

$$\mathcal{L}_{\text{online-fixing}}(\theta) = \mathbb{E}_{x \sim \mathcal{D}}[\mathcal{L}_{\text{GRPO}}(x; \theta)] + \mathbb{E}_{x \sim \mathcal{D}, y \sim \pi_\theta(\cdot | x)}[\mathbf{1}[r(y) = 0] \mathcal{L}_{\text{GRPO}}(z; \theta)]. \quad (8)$$

The *resample-only* control keeps the same second term, but replaces  $z = \phi(x, y)$  with a fresh retry prompt that omits the failed code and execution statistics.

The prompt  $z$  is constructed using the following template.

#### System Prompt

You are a helpful AI assistant. You always reason before responding, using the following format:

```
<think>
your internal reasoning
</think>
your external response
```

#### User Prompt Template

Solve the following competitive programming question.

Question:  
{problem statement}

For your reference, here is a previous solution attempt that failed some unit tests:

```
```python
{failed code}
```
```

Unit tests execution statistics:  
{exec\_stats}

You may use this code as reference or inspiration, but you are free to write a completely new solution. Make sure to avoid repeating the same errors. Consider:

- FAILURE or EXCEPTION cases: edge cases, boundary values, off-by-one errors, or logic flaws.
- TIMEOUT cases: algorithm complexity, better data structures, or redundant computations.

Your code should be enclosed in triple backticks like so: ```python YOUR CODE HERE```. Use the backticks for your code only.

### G.3 Main Figure

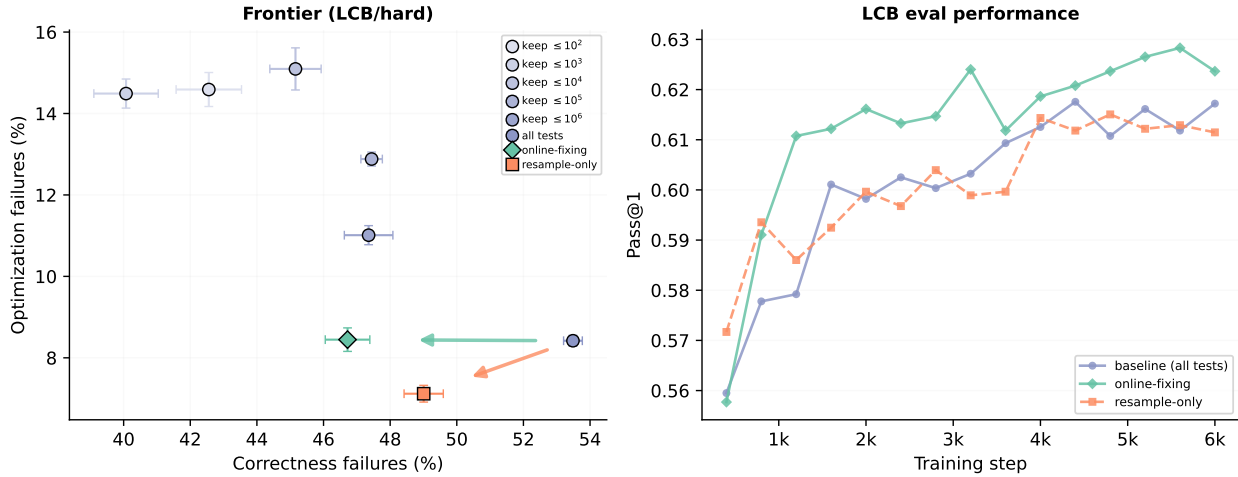


**Figure 29** Failure-conditioned correction compared with a compute-matched resample-only control on 32B pure reasoning setting. **Left:** on the original code-generation task, both online-fixing (green diamond) and the resample-only control (orange square) reduce optimization failures relative to standard RL checkpoints (circles), but only online-fixing simultaneously reduces correctness failures. Arrows indicate the shift from the no-filter baseline. **Right:** pass@1 on LCB over training for the original code-generation task; the online-fix curve is ahead earlier in training, though the gap narrows later. See Appendix G.4 for the full per-setting tables.

### G.4 Additional Online-Fixing Results

The sections in the main text establish that the trade-off is robust across settings and scales. Longer training can still push the frontier outward, but a sharper question is whether a different use of the same training budget can improve it at matched trainer compute. The *online-fixing* experiments in this appendix address that question by changing how worker-side sampling is spent after failures.

Online-fixing changes two aspects of training at once: it spends more worker-side sampling on problems the model currently fails on, and it augments the online prompt distribution with failure-conditioned prompts. The *resample-only* control matches the extra retry budget without adding failure context, so it isolates the value of the failure-conditioned prompt itself.

A key property of the design is that it keeps trainer compute fixed while increasing worker compute adaptively after failures. The computation graph is cut at the boundary between the failed rollout and the fixing prompt, so the fixing rollout is treated as a new sample rather than a second turn in the same trajectory. The trainer therefore processes the same number of gradient steps regardless of how many failure-conditioned rollouts are spawned.

**Table 2** Pass rate and self-fixing solve rate for additional worker compute comparison (32B pure-reasoning setting), including online-fixing and its resample-only control, reported on LCB/hard and full LCB. Numbers are averaged from the last three evaluations.

|               | LCB/hard        |                 | LCB             |                 | LCB/hard (fix)  |                 | LCB (fix)       |                 |
|---------------|-----------------|-----------------|-----------------|-----------------|-----------------|-----------------|-----------------|-----------------|
|               | pass@1          | pass@5          | pass@1          | pass@5          | fix@1           | fix@5           | fix@1           | fix@5           |
| Baseline      | 29.2±0.7        | 46.5±1.4        | 61.5±0.2        | 72.7±0.8        | 14.1±1.4        | 33.5±0.5        | 22.2±3.4        | 43.7±2.9        |
| Resample only | 30.8±0.3        | <b>48.4±0.7</b> | 61.2±0.1        | <b>73.3±0.4</b> | 14.2±0.5        | 34.9±1.3        | 20.8±0.5        | 44.1±0.7        |
| Online-fixing | <b>30.9±1.1</b> | 45.8±0.6        | <b>62.6±0.2</b> | 72.8±0.3        | <b>17.9±1.3</b> | <b>37.5±1.0</b> | <b>28.1±1.0</b> | <b>49.1±0.9</b> |

**Table 3** Pass rate and self-fixing solve rate for additional worker compute comparison (7B pure-reasoning setting), including online-fixing and its resample-only control, reported on LCB/hard and full LCB. Numbers are averaged from the last three evaluations.

|               | LCB/hard              |                       | LCB                   |                       | LCB/hard (fix)       |                       | LCB (fix)             |                       |
|---------------|-----------------------|-----------------------|-----------------------|-----------------------|----------------------|-----------------------|-----------------------|-----------------------|
|               | pass@1                | pass@5                | pass@1                | pass@5                | fix@1                | fix@5                 | fix@1                 | fix@5                 |
| Baseline      | 13.7 $\pm$ 0.6        | 27.4 $\pm$ 0.9        | 45.7 $\pm$ 0.1        | 59.6 $\pm$ 0.3        | 7.4 $\pm$ 0.5        | 19.5 $\pm$ 0.9        | 15.4 $\pm$ 1.9        | 34.2 $\pm$ 2.2        |
| Resample only | <b>14.3</b> $\pm$ 0.3 | <b>29.2</b> $\pm$ 1.0 | 45.6 $\pm$ 0.3        | <b>60.6</b> $\pm$ 0.7 | 7.9 $\pm$ 0.5        | 21.9 $\pm$ 1.5        | 17.2 $\pm$ 0.9        | 37.2 $\pm$ 0.1        |
| Online-fixing | 14.2 $\pm$ 1.0        | 28.0 $\pm$ 0.3        | <b>45.9</b> $\pm$ 0.6 | 60.1 $\pm$ 0.1        | <b>9.7</b> $\pm$ 0.7 | <b>22.8</b> $\pm$ 0.7 | <b>18.5</b> $\pm$ 0.6 | <b>38.2</b> $\pm$ 0.5 |

**Table 4** Pass rate and self-fixing solve rate for additional worker compute comparison (32B tool-interleaved setting), including online-fixing and its resample-only control, reported on LCB/hard and full LCB. Numbers are averaged from the last three evaluations.

|               | LCB/hard              |                       | LCB                   |                       | LCB/hard (fix)        |                       | LCB (fix)             |                       |
|---------------|-----------------------|-----------------------|-----------------------|-----------------------|-----------------------|-----------------------|-----------------------|-----------------------|
|               | pass@1                | pass@5                | pass@1                | pass@5                | fix@1                 | fix@5                 | fix@1                 | fix@5                 |
| Baseline      | 34.6 $\pm$ 1.3        | 52.0 $\pm$ 1.3        | 64.5 $\pm$ 0.7        | 75.6 $\pm$ 0.6        | 15.5 $\pm$ 0.5        | 36.2 $\pm$ 1.9        | 20.3 $\pm$ 1.3        | 42.7 $\pm$ 2.1        |
| Resample only | 34.7 $\pm$ 0.9        | <b>54.8</b> $\pm$ 2.5 | 64.3 $\pm$ 0.7        | <b>77.6</b> $\pm$ 1.4 | 13.4 $\pm$ 2.4        | 32.7 $\pm$ 2.7        | 19.8 $\pm$ 3.3        | 41.7 $\pm$ 4.0        |
| Online-fixing | <b>36.2</b> $\pm$ 1.0 | 52.9 $\pm$ 1.8        | <b>65.2</b> $\pm$ 0.4 | 75.9 $\pm$ 0.9        | <b>16.3</b> $\pm$ 1.5 | <b>36.3</b> $\pm$ 1.7 | <b>21.2</b> $\pm$ 0.7 | <b>43.9</b> $\pm$ 0.6 |

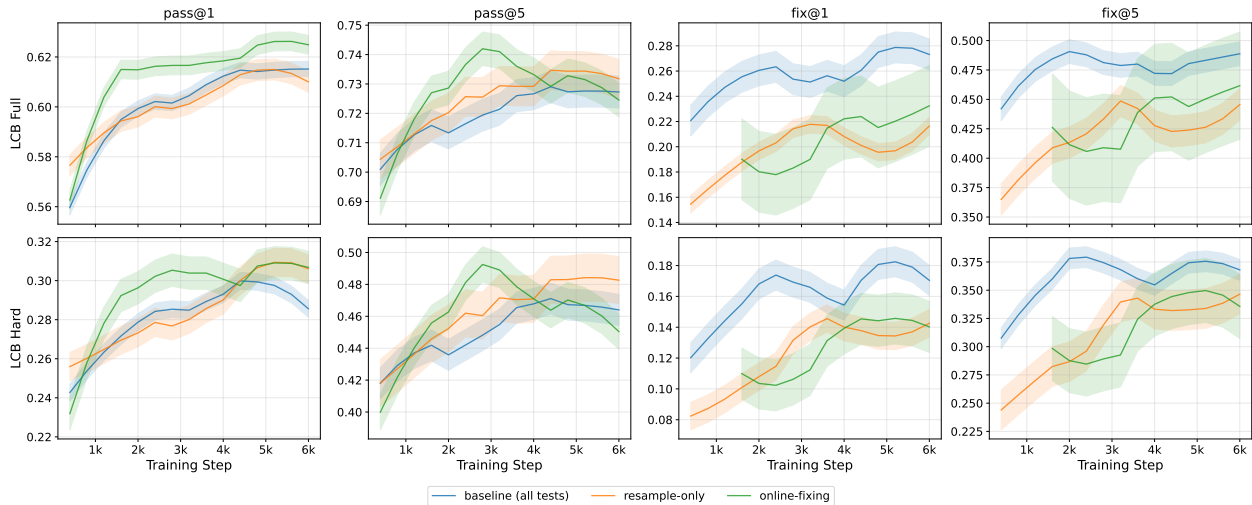


**Figure 30** Evaluation curves for the 32B pure-reasoning runs over the first 6k training steps. **Top row:** full LCB evaluation set. **Bottom row:** hard subset only. Columns show pass@1, pass@5, fix@1, and fix@5 respectively. Online-fixing matches or slightly exceeds the baseline and resample-only control on the standard code-generation metrics (pass@1, pass@5), while showing a clear advantage on the self-repair metrics (fix@1, fix@5).

Beyond the original code-generation metrics, online-fix training also strengthens the self-fixing task throughout training. Figure 30 shows that the online-fix model consistently outperforms both the resample-only control and the baseline on fix@1 and fix@5.

## H Weight-Space Geometry

This appendix characterizes the weight-space direction that separates the two RL endpoints along three axes: the singular-value spectrum of each layer’s weight difference (Section H.1), the distribution of squared weight change across layers (Section H.2), and layer stitching experiments that isolate causal contributions to behavior (Section H.3).

The central finding is a dissociation. RL modifies every layer by similar magnitudes and in high-dimensional directions: the top 10 singular values explain only 10 to 19% of the variance within each layer (Section H.1), and the total squared weight change is nearly uniform across layers 2 through 63 (Section H.2). Yet behavioral sensitivity is concentrated in the middle of the network. Layer stitching shows that the first and last quarter of layers (0 to 15 and 48 to 63) are nearly inert, while the middle half (16 to 47) carries the full trade-off shift, with layers 24 to 31 accounting for roughly half of it (Section H.3).

### H.1 SVD Spectrum

For each weight matrix in the 32B 64-layer model, we compute the SVD of  $\delta = \theta_{\text{high}} - \theta_{\text{low}}$  and measure the cumulative variance explained by the top  $k$  singular values. Figure 31 shows the result, normalized by the rank of each matrix. No component type is low-rank: the top 10 singular values of each layer’s difference explain only 10 to 19% of variance, and even at 20% of rank no component exceeds 80% explained variance.

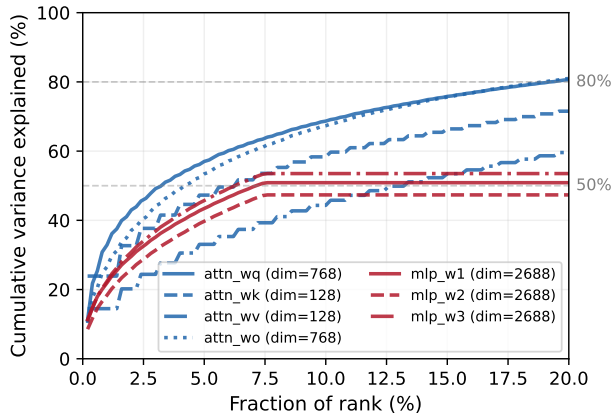


**Figure 31** Cumulative variance explained by the top singular values of the weight difference  $\delta = \theta_{\text{high}} - \theta_{\text{low}}$ , averaged across layers and normalized by rank. Attention matrices concentrate variance faster than MLP matrices, but neither is low-rank: at 20% of rank, no component type exceeds 80% explained variance.

### H.2 Per-Layer Variance Distribution

We define the *variance ratio* of layer  $\ell$  as the fraction of total squared change ( $\|\delta\|^2$  summed across all parameters) attributable to that layer; under a uniform distribution each of 64 layers would contribute 1.56%. Figure 32 shows that the variance ratio is nearly uniform across layers 2 through 63, with only layers 0 and 1 markedly below baseline.

### H.3 Layer Stitching

The previous two analyses show that weight changes are distributed and high-dimensional, but this does not imply uniform causal importance. We construct Frankenstein models by taking layers 0 through  $k-1$  from  $\theta_{\text{high}}$  and layers  $k$  through 63 from  $\theta_{\text{low}}$  (and vice versa), sweeping cutpoints  $k \in \{0, 16, 24, 32, 48, 64\}$ . We additionally test block swaps of layers 24 to 31 (8 layers) and 16 to 47 (32 layers).

All stitched models remain on the trade-off curve, with success rates in the 32.8 to 37.4% band (Figure 33). The first and last quarter of layers are nearly inert: cutpoints at  $k=16$  and  $k=48$  shift timeout counts by

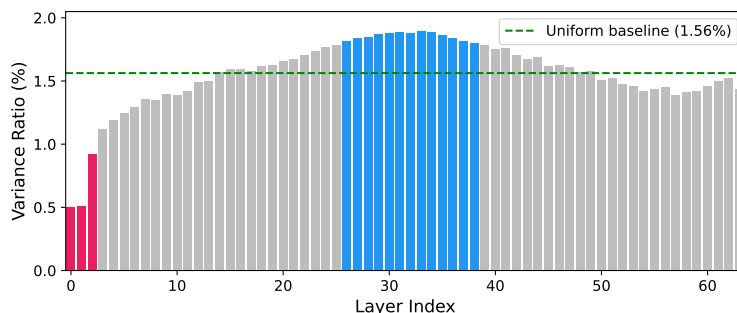


**Figure 32** Per-layer variance ratio (fraction of total squared weight change). The dashed line marks the uniform baseline (1.56% per layer). Layers 0-1 (red) are markedly below baseline; layers 24-36 (blue) are mildly above. The distribution is otherwise close to uniform.

fewer than 6 relative to the endpoints. The middle layers carry the full behavioral shift. Swapping layers 24 to 31 alone (12.5% of the network) accounts for roughly half the timeout shift; swapping layers 16 to 47 reproduces or slightly overshoots the full shift (Figure 34).

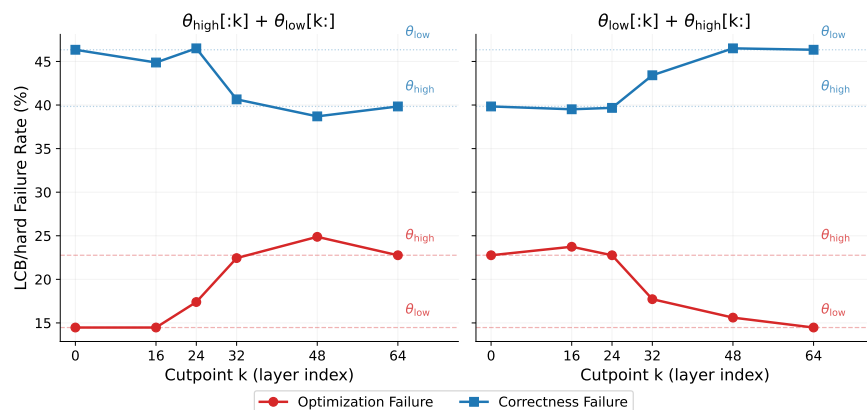


**Figure 33** Layer stitching (Frankenstein models): optimization failure rate and correctness failure rate on LCB/hard as a function of cutpoint  $k$ . **Left:** layers 0 through  $k-1$  from  $\theta_{\text{high}}$ , layers  $k$  through 63 from  $\theta_{\text{low}}$ . **Right:** the reverse direction. Dashed lines mark the endpoint levels. The behavioral transition is concentrated in the middle layers (roughly 16-48); edge layers are nearly inert.

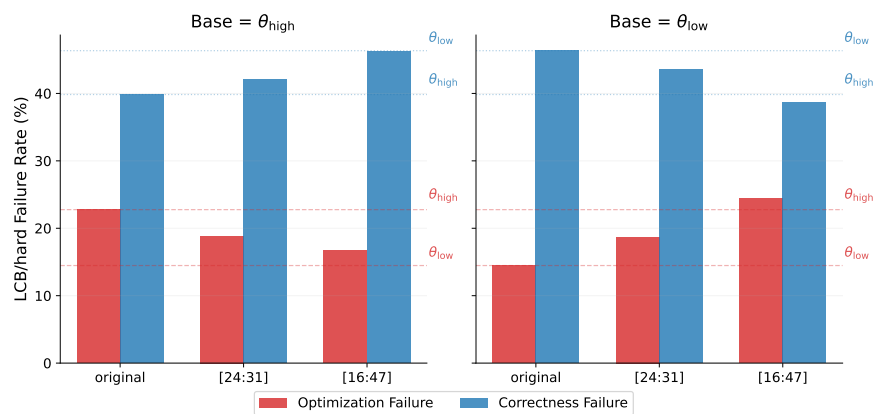


**Figure 34** Block swap: replacing a contiguous range of middle layers in one endpoint with the corresponding layers from the other. **Left:**  $\theta_{high}$  base with  $\theta_{low}$  layers swapped in. **Right:**  $\theta_{low}$  base with  $\theta_{high}$  layers swapped in. Swapping layers 16-47 (half the model) nearly reproduces the full behavioral shift; swapping layers 24-31 (8 layers) produces a partial shift, confirming that a dense core of middle layers controls the trade-off.

# I Error Taxonomy Validation with Extended Reclassification

A submission that exceeds resource limits does not necessarily implement a correct algorithm; it may contain a bug masked by the resource limit. To assess the sensitivity of our results to this ambiguity, we apply a two-stage reclassification protocol to every submission originally labeled as an optimization failure. We detail the protocol in Section I, with Figure 35 showing the comparison of the extended reclassification and the raw sandbox signal used in the main text. Section I.2 reveals one interesting finding: a substantial fraction of timed-out submissions are in fact memory-exhaustion failures masked by the time limit. Whether a slow submission will eventually exhaust memory or time is fundamentally difficult to determine without running it to completion, which we believe explains why most existing work aggregates both failure modes into a single timeout category.

## I.1 Reclassification Protocol

**Stage 1: extended re-evaluation.** We re-execute each submission labeled as optimization error with a  $100\times$  time budget. Under this extended budget, submissions fall into one of four categories: (i) *all-pass*, confirming a correct but algorithmically slow implementation; (ii) *wrong answer*, revealing a correctness bug that was masked by the original time limit; (iii) *out of memory*, indicating that the submission is memory-intensive and the original timeout pre-empted the true failure mode; or (iv) *still timeout*, remaining ambiguous.

Table 5 reports the breakdown for the high-coverage training condition (all test cases included) across all three inference settings. A substantial fraction of optimization failures are confirmed correct under the extended budget (27-40% across settings and thresholds), while out-of-memory errors account for 5-14% of originally timed-out submissions. Table 5 reports the full breakdown.

**Table 5** Stage 1 re-evaluation outcomes (% of timed-out submissions) under a  $100\times$  time budget. Each column corresponds to one test-coverage threshold; each row group to one inference setting. “Total” is the number of submissions originally labeled as optimization failures.

|                       | $\leq 10^2$ | $\leq 10^3$ | $\leq 10^4$ | $\leq 10^5$ | $\leq 10^6$ | all   |
|-----------------------|-------------|-------------|-------------|-------------|-------------|-------|
| <i>Pure Reasoning</i> |             |             |             |             |             |       |
| Total                 | 153         | 167         | 157         | 158         | 124         | 104   |
| All-pass              | 37.3%       | 31.1%       | 36.9%       | 39.9%       | 40.3%       | 34.6% |
| Wrong answer          | 3.3%        | 5.4%        | 4.5%        | 0.6%        | 2.4%        | 2.9%  |
| Out of memory         | 9.2%        | 4.8%        | 7.6%        | 7.6%        | 5.6%        | 8.7%  |
| Still timeout         | 47.1%       | 53.9%       | 43.3%       | 50.0%       | 46.8%       | 49.0% |
| Other                 | 3.3%        | 4.8%        | 7.6%        | 1.9%        | 4.8%        | 4.8%  |
| <i>Tool Use</i>       |             |             |             |             |             |       |
| Total                 | 140         | 139         | 126         | 109         | 99          | 89    |
| All-pass              | 22.1%       | 17.3%       | 15.9%       | 22.0%       | 33.3%       | 36.0% |
| Wrong answer          | 4.3%        | 3.6%        | 5.6%        | 3.7%        | 3.0%        | 11.2% |
| Out of memory         | 10.0%       | 7.2%        | 14.3%       | 11.9%       | 9.1%        | 10.1% |
| Still timeout         | 57.9%       | 68.3%       | 58.7%       | 58.7%       | 51.5%       | 41.6% |
| Other                 | 5.7%        | 3.6%        | 5.6%        | 3.7%        | 3.0%        | 1.1%  |
| <i>Agentic Coding</i> |             |             |             |             |             |       |
| Total                 | 139         | 131         | 114         | 89          | 80          | 69    |
| All-pass              | 26.6%       | 26.7%       | 31.6%       | 25.8%       | 27.5%       | 27.5% |
| Wrong answer          | 2.9%        | 4.6%        | 2.6%        | 3.4%        | 3.8%        | 5.8%  |
| Out of memory         | 7.2%        | 6.1%        | 9.6%        | 6.7%        | 10.0%       | 13.0% |
| Still timeout         | 56.8%       | 55.7%       | 49.1%       | 60.7%       | 53.8%       | 52.2% |
| Other                 | 6.5%        | 6.9%        | 7.0%        | 3.4%        | 5.0%        | 1.4%  |

**Stage 2: LLM judgment.** For submissions that still exceed resource limits or sandbox error after Stage 1 (the “still timeout”, “out of memory” and “Other” rows), we query a strong model, Claude-4.5-Sonnet with

multiple generations and majority voting to binary classify whether the implementation is logically correct but algorithmically naive, or whether it contains a correctness bug. Table 6 reports the fraction of optimization failures reclassified as correctness failures after combining both stages, across all settings and thresholds. Crucially, the number of successful submissions is unchanged in every condition: reclassification only moves submissions from the optimization failure category to correctness failure, never to success.

**Table 6** Final reclassification outcome after both stages (% of original optimization failures). The two rows sum to 100% for each condition.

|                              | $\leq 10^2$ | $\leq 10^3$ | $\leq 10^4$ | $\leq 10^5$ | $\leq 10^6$ | all   |
|------------------------------|-------------|-------------|-------------|-------------|-------------|-------|
| <i>Pure Reasoning</i>        |             |             |             |             |             |       |
| Reclass. correctness failure | 17.6%       | 16.2%       | 15.9%       | 17.1%       | 15.3%       | 20.2% |
| Remain optimization failure  | 82.4%       | 83.8%       | 84.1%       | 82.9%       | 84.7%       | 79.8% |
| <i>Tool Use</i>              |             |             |             |             |             |       |
| Reclass. correctness failure | 5.0%        | 10.1%       | 13.5%       | 15.6%       | 6.1%        | 22.5% |
| Remain optimization failure  | 95.0%       | 89.9%       | 86.5%       | 84.4%       | 93.9%       | 77.5% |
| <i>Agentic Coding</i>        |             |             |             |             |             |       |
| Reclass. correctness failure | 20.1%       | 27.5%       | 27.2%       | 19.1%       | 22.5%       | 31.9% |
| Remain optimization failure  | 79.9%       | 72.5%       | 72.8%       | 80.9%       | 77.5%       | 68.1% |

**Robustness of the trade-off.** Figure 35 compares the trade-off curve before and after reclassification across all three inference settings and all six test-coverage thresholds. In each panel, raw sandbox labels (solid) and reclassified labels (dashed) trace nearly identical frontiers. The reclassified curve shifts slightly toward higher correctness failure rates, as expected from unmasking hidden bugs, but the shape and slope of the frontier are preserved. Since the relative orders are preserved, the two labeling schemes agree closely and can be seen as a global shift of the trade-off curve, we use raw sandbox labels throughout the main paper to avoid the computational cost of running the full reclassification pipeline at every evaluation checkpoint.

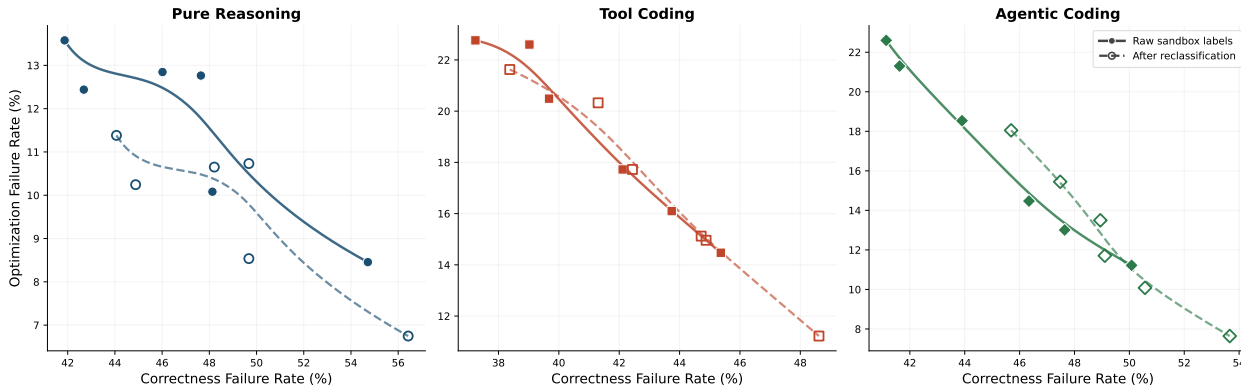


**Figure 35** Trade-off curves under raw sandbox labels (solid) versus reclassified labels (dashed) for pure reasoning (left), tool coding (center), and agentic coding (right). Each point is one training checkpoint under a fixed test-coverage threshold. The two labeling schemes produce nearly overlapping frontiers, validating the use of raw labels in the main paper.

## 1.2 Hidden Memory Exhaustion in Timeout Labels

Standard competitive-programming evaluation pipelines enforce both a time limit and a memory limit, but when a submission exceeds the time limit first, the sandbox reports a timeout regardless of whether the code would also have exhausted memory. Memory exhaustion is therefore aggregated into the timeout category, making it invisible in downstream analysis.

Our extended re-evaluation (Stage 1 of the reclassification protocol, Appendix I) surfaces this hidden failure

mode. Under the  $100\times$  time budget, 5% to 14% of originally timed-out submissions across all settings and thresholds terminate with an out-of-memory error rather than a wrong answer or a continued timeout (Table 5).

These submissions implement memory-intensive algorithms (e.g., building large lookup tables or storing full search trees) whose true failure mode is masked by the shorter time limit. Since competitive-programming benchmarks are the primary training and evaluation environment for code RL, this conflation means that a non-trivial fraction of what existing work treats as “slow but possibly correct, i.e., timeout error” code is in fact code that would crash from memory exhaustion even given enough time. Disentangling time and memory failures may be important for designing reward signals that distinguish algorithmic efficiency from implementation correctness.

## J Case Studies: Full Trajectories Across the Frontier

We present two case studies from the tool-coding setting that concretely illustrate the correctness–efficiency trade-off. Both come from LCB/hard problems that are *differentially solved* across the interpolation axis. For each, we show the *complete multi-turn trajectory* of a representative rollout from the two RL endpoints:

- **Low-coverage** ( $\alpha=0$ ; CodeContestsPlus with test inputs  $\leq 10^2$ ): trained against small-input tests only.
- **High-coverage** ( $\alpha=1$ ; CodeContestsPlus unfiltered): trained against the full test suite including large-input stress tests.

Both checkpoints are evaluated at step 3600 with 5 samples per problem. Thinking blocks are truncated for space; all code and tool output are shown verbatim.

### J.1 Case 1: Falling Bars (hard/770)

**Problem.** Given an  $H \times W$  grid with  $N$  horizontal bars, simulate gravity: at each time step, bars are processed in index order  $i=1, \dots, N$ ; bar  $i$  moves down one row if all cells directly below it are unoccupied. Output each bar’s final row at  $t=10^{100}$ . Constraints:  $H, W, N \leq 2 \times 10^5$ .

**Results.** Low-coverage: **5/5 success**. High-coverage: **0/5 success** (all wrong answer, e.g. 2,3,4,4 instead of 2,4,3,4).

#### J.1.1 Low-coverage trajectory (success)

Assistant – Turn 1 (python-io): Reverse-order single pass

```
<think>
... The key insight here is that once a bar stops moving, it
might block other bars from moving. So, the order in which bars
are processed matters. ... One approach is to ... process bars
in reverse index order, tracking the highest occupied row per
column. ...
</think>

<tool: python-io>
<code>
bars.sort(key=lambda x: -x[3]) # reverse index order
occupied = {} # column -> highest occupied row
result = [0] * N
for R, C, L, idx in bars:
    columns = list(range(C, C + L))
    max_row = H
    for c in columns:
        h = occupied.get(c, 0)
        current_max = h - 1 if h else H
        max_row = min(max_row, current_max)
    result[idx] = max_row
    for c in columns:
        occupied[c] = max(occupied.get(c, 0), max_row)
for row in result:
    print(row)
</code>
<stdin>4 4 4
1 2 3
3 2 2
2 1 2
2 4 1</stdin>
</tool>
```

Tool Response

```
completed. [stdout]2
3
4
4[/stdout]

<budget> Remaining turns: 5, Remaining tokens: 45462 </budget>
```

**Turns 2–3.** Same reverse-order approach with minor refactors; output remains 2,3,4,4. Stress test confirms the bug.

#### Assistant – Turn 4 (python-io): Forward order with static lookahead

```
<think>
... The reverse processing approach is fundamentally flawed for
this problem. Let me think differently. Perhaps the correct
approach is to process bars in original order and also check
initial positions of unprocessed bars ...
</think>

<tool: python-io>
<code>
for R, C, L, idx in bars: # forward order now
    columns = list(range(C, C+L))
    min_max_row = H
    for c in columns:
        current_h = occupied.get(c, 0)
        candidate = current_h - 1 if current_h else H
        min_max_row = min(min_max_row, candidate)
    # Also check initial positions of unprocessed bars
    for j in range(N):
        if j > idx: # unprocessed (higher index)
            r_j, c_j, l_j, _ = bars[j]
            if r_j > R: # bar j is initially below
                overlap_start = max(C, c_j)
                overlap_end = min(C + L - 1, c_j + l_j - 1)
                if overlap_start <= overlap_end:
                    min_max_row = min(min_max_row, r_j)
    result[idx] = min_max_row
    ...
</code>
<stdin>4 4 4
1 2 3
3 2 2
2 1 2
2 4 1</stdin>
</tool>
```

#### Tool Response

```
completed. [stdout]2
1
1
1[/stdout]

<budget> Remaining turns: 2, Remaining tokens: 39584 </budget>
```

#### Assistant – Turn 5 (python-io): Brute-force simulation |←| pivot

```
<think>
... The code now produces output 2, 1, 1, 1, which is even
worse. Clearly, this approach is incorrect. The issue is that
checking the initial positions of unprocessed bars is not
sufficient, as those bars may move down in subsequent time
steps. ... Given the need to provide a correct solution, I'll
try a direct simulation approach.
</think>

<tool: python-io>
<code>
current_rows = [R for R, _, _, _ in bars]
occupied = [set() for _ in range(H+2)]
for i in range(N):
    R, C, L, _ = bars[i]
    for c in range(C, C+L):
        occupied[R].add(c)
changed = True
while changed:
    changed = False
    for i in range(N):
        R, C, L, _ = bars[i]
        current_R = current_rows[i]
        if current_R == H:
            continue
```

```

    can_move = True
    for c in range(C, C+L):
        if c in occupied[current_R + 1]:
            can_move = False
            break
    if can_move:
        for c in range(C, C+L):
            occupied[current_R].remove(c)
            current_rows[i] += 1
        for c in range(C, C+L):
            occupied[current_R + 1].add(c)
        changed = True
for row in current_rows:
    print(row)
</code>
<stdin>4 4 4
1 2 3
3 2 2
2 1 2
2 4 1</stdin>
</tool>

```

### Tool Response

```

completed. [stdout]2
4
3
4[/stdout]

<budget> Remaining turns: 1, Remaining tokens: 38194 </budget>

```

**Turn 6.** Stress-tests the simulation on  $N=200,000$ ; encounters a `KeyError` on random overlapping bars but the core algorithm is correct.

### Assistant – Final Submission

```

<think>
The simulation approach produces the correct output for the
sample input. The stress test revealed a KeyError when removing
a column, likely due to overlapping bars in the random test.
Given the time constraints, I'll submit the simulation code.
</think>

```

*(submits the simulation code from Turn 5)*

## J.1.2 High-coverage trajectory (wrong answer)

### Assistant – Turn 1 (python-io): Segment tree, reverse order

```

<think>
... I need to find a way to model the dependencies between
bars. ... Let me consider processing bars in reverse index
order, using a segment tree to track the minimum occupied row
for each column range ...
</think>

<tool: python-io>
<code>
import sys, math

def main():
    data = sys.stdin.read().split()
    H, W, N = int(data[0]), int(data[1]), int(data[2])
    bars = []
    idx = 3
    for _ in range(N):
        R, C, L = int(data[idx]), int(data[idx+1]), int(data[idx+2])
        bars.append((R, C, L)); idx += 3
    result = [0]*N
    size = 1
    while size < W: size <= 1
    min_row = [math.inf] * (2 * size)

```

```

def update(l, r, val):
    l += size - 1; r += size - 1
    while l <= r:
        if l % 2 == 1: min_row[l] = min(min_row[l], val); l += 1
        if r % 2 == 0: min_row[r] = min(min_row[r], val); r -= 1
        l >>= 1; r >>= 1
def query(l, r):
    res = math.inf; l += size - 1; r += size - 1
    while l <= r:
        if l % 2 == 1: res = min(res, min_row[l]); l += 1
        if r % 2 == 0: res = min(res, min_row[r]); r -= 1
        l >>= 1; r >>= 1
    return res
for i in reversed(range(N)):
    R, C, L = bars[i]
    current_min = query(C, C + L - 1)
    new_R = min(H, current_min - 1) if current_min != math.inf else H
    result[i] = new_R
    update_val = new_R + 1 if new_R < H else math.inf
    update(C, C + L - 1, update_val)
for r in result: print(r)
main()
</code>
<stdin>4 4 4
1 2 3
3 2 2
2 1 2
2 4 1</stdin>
</tool>

```

### Tool Response

```

completed. [stdout]4
4
4
4[/stdout]

<budget> Remaining turns: 5, Remaining tokens: 46198 </budget>

```

Turn 2 (python-io). Fixes segment-tree indexing to 0-based; output unchanged: 4,4,4,4.

### Assistant – Turn 3 (python-stress): Assertion failure

```

<think>
... The output is still incorrect. All bars are at row 4, but
the correct output should be 2, 4, 3, 4. The issue must be in
the segment tree implementation or the logic of updating ...
</think>

<tool: python-stress>
... (same reverse-order segment tree code)
result = solve(H, W, N, bars)
print("Result:", result)
print("Expected:", expected)
assert result == expected, f"Test failed: {result} != {expected}"
</tool>

```

### Tool Response

```

completed. [stdout]Result: [4, 4, 4, 4]
Expected: [2, 4, 3, 4][/stdout]
[stderr]AssertionError: Test failed: [4, 4, 4, 4] != [2, 4, 3, 4][/stderr]

```

### Assistant – Turn 4 (python-io): Plain array, still reverse order

```

<think>
... The stress test confirms that the current approach is
incorrect. ... Let me simplify and use a plain array instead of
a segment tree, but keep the reverse processing order ...
</think>

<tool: python-io>

```

```

<code>
min_row = [H+1] * (W + 2) # 1-based
for i in reversed(range(N)):
    R, C, L = bars[i]
    current_min = min(min_row[C : C+L])
    if current_min == H+1:
        new_R = H
    else:
        new_R = min(H, current_min - 1)
    result[i] = new_R
    for c in range(C, C+L):
        if min_row[c] > new_R:
            min_row[c] = new_R
</code>
<stdin>4 4 4
1 2 3
3 2 2
2 1 2
2 4 1</stdin>
</tool>

```

### Tool Response

```

completed. [stdout]2
3
4
4[/stdout]

<budget> Remaining turns: 2, Remaining tokens: 40695 </budget>

```

**Turn 5 (python-io).** Changes update value to `new_R + 1`; output regresses to 4,4,4,4.

**Turn 6 (python-io).** Reverts to `new_R`; output returns to 2,3,4,4—still wrong. The model is stuck cycling between two incorrect variants.

### Assistant – Final Submission

```

<think>
... The output is still [2, 3, 4, 4], which is close but not
correct. Bar 2 should be at row 4, not row 3. The fundamental
issue is in how the reverse processing handles the interaction
between bars ...
</think>

(submits the reverse-order min_row code from Turn 4; wrong answer)

```

### J.1.3 Interpretation

Both models initially try the same efficient reverse-processing idea. The low-coverage model *pivots* to brute-force simulation when it fails (Turn 5); the high-coverage model spends all 6 tool turns on variants of the single-pass approach, never attempting simulation. The low-coverage model’s willingness to fall back to a correct-but-slow algorithm is the difference between 5/5 success and 0/5.

## J.2 Case 2: Largest Palindrome Divisible by $K$ (hard/680)

**Problem.** Given  $n$  and  $k$  ( $1 \leq n \leq 10^5$ ,  $1 \leq k \leq 9$ ), find the largest  $n$ -digit palindrome divisible by  $k$ .

**Results.** Low-coverage: **0/5 success** (all timeout). High-coverage: **1/5 success** (3 timeout, 1 wrong answer).

## J.2.1 Low-coverage trajectory (timeout)

### Assistant – Turn 1 (python-io): Brute-force decrement

```
<think>
... The task is to find the largest n-digit number that is both
a palindrome and divisible by k. ... Start from the largest
palindrome and work downward until we find one divisible by k.
</think>

<tool: python-io>
<code>
class Solution:
    def largestPalindrome(self, n: int, k: int) -> str:
        m = (n + 1) // 2
        first_half = '9' * m
        while True:
            if n % 2 == 0:
                palindrome = first_half + first_half[::-1]
            else:
                palindrome = first_half + first_half[:-1][::-1]
            if self.is_divisible(palindrome, k):
                return palindrome
            new_first_half = self.decrement_first_half(first_half)
            if new_first_half is None:
                return ""
            first_half = new_first_half

    def is_divisible(self, s, k):
        mod = 0
        for c in s:
            mod = (mod * 10 + int(c)) % k
        return mod == 0

    def decrement_first_half(self, s):
        s_list = list(s)
        i = len(s_list) - 1
        carry = 1
        while i >= 0 and carry:
            digit = int(s_list[i])
            if digit - carry >= 0:
                s_list[i] = str(digit - carry)
                carry = 0
            else:
                s_list[i] = '9'
                carry = 1
            i -= 1
        if s_list[0] == '0':
            return None
        return ''.join(s_list)
</code>
<stdin>3
5</stdin>
</tool>
```

### Tool Response

```
completed.
<budget> Remaining turns: 5, Remaining tokens: 51467 </budget>
```

**Turn 2.** Tests second example (n=1,k=4); passes with output "8".

### Assistant – Turn 3 (python-stress): Large input test

```
<think>
... Let me test with large inputs to check performance. For
n=100000, the first_half has 50000 digits ...
</think>

<tool: python-stress>
...
test_cases = [(3, 5), (1, 4), (5, 6), (2, 2), (100000, 9)]
for n, k in test_cases:
```

```

start = time.time()
result = Solution().largestPalindrome(n, k)
elapsed = time.time() - start
print(f"n={n}, k={k}: time={elapsed:.3f}s")
</tool>

```

### Tool Response

error: EXECUTION\_TIMEOUT after 60 seconds

### Assistant – Final Submission

```

<think>
... The stress test timed out for n=100000. The brute-force
approach is too slow for large inputs. But given the time
constraints, I'll submit this solution.
</think>

```

*(submits brute-force decrement code; timeout on hidden tests)*

## J.2.2 High-coverage trajectory (success)

### Assistant – Turn 1 (python-io): Optimized remainder, still brute-force

```

<think>
... Let me start by considering the structure of the palindrome.
For an n-digit number, each half-digit contributes to two
symmetric positions. I can precompute the coefficient of each
position modulo k to speed up the divisibility check ...
</think>

<tool: python-io>
<code>
class Solution:
    def largestPalindrome(self, n: int, k: int) -> str:
        if k == 1: return '9' * n
        m = (n + 1) // 2 if n % 2 else n // 2
        pow10_mod = [1] * n
        for i in range(1, n):
            pow10_mod[i] = (pow10_mod[i-1] * 10) % k
        def get_remainder(s):
            remainder = 0
            for i in range(len(s)):
                digit = int(s[i])
                if n % 2 == 0 or i < len(s) - 1:
                    coeff = (pow10_mod[n-1-i] + pow10_mod[i]) % k
                else:
                    coeff = pow10_mod[n-1-i] % k
                remainder = (remainder + digit * coeff) % k
            return remainder
        first_half = '9' * m
        while True:
            if get_remainder(first_half) == 0:
                if n % 2:
                    return first_half + first_half[::-1][::-1]
                else:
                    return first_half + first_half[::-1]
            s_list = list(first_half)
            i = len(s_list) - 1
            while i >= 0 and s_list[i] == '0':
                s_list[i] = '9'; i -= 1
            if i >= 0: s_list[i] = str(int(s_list[i]) - 1)
            first_half = ''.join(s_list)
            if first_half[0] == '0': return "0" * n

</code>
<stdin>3
5</stdin>
</tool>

```

### Tool Response

```
completed.  
<budget> Remaining turns: 5, Remaining tokens: 48438 </budget>
```

### Assistant – Turn 2 (python-stress): Discovers timeout

```
<think>  
... Let me test with large inputs to verify performance ...  
</think>  
  
<tool: python-stress>  
test_cases = [(10**5, 9), (10**5, 2), (10**5, 5)]  
for n, k in test_cases:  
    start = time.time()  
    result = Solution().largestPalindrome(n, k)  
    elapsed = time.time() - start  
    print(f"n={n}, k={k} Time: elapsed:3fs")</tool>
```

### Tool Response

```
error: EXECUTION_TIMEOUT after 60 seconds  
<budget> Remaining turns: 4, Remaining tokens: 46406 </budget>
```

### Assistant – Turn 3 (python-io): DP with backward reachability |←| pivot

```
<think>  
... The stress test timed out for large n=1e5. The main issue  
is the decrement loop -- for large n, the first_half can be up  
to 5e4 digits, and decrementing each time is O(m). We need a  
fundamentally different approach. ...  
  
Since k <= 9, the remainder modulo k has at most 9 possible  
values. For each half-digit position, we can precompute its  
coefficient mod k. Then use DP: compute which remainders are  
reachable from each suffix of the half-string, and greedily  
assign the largest valid digit at each position.  
</think>  
  
<tool: python-io>  
<code>  
class Solution:  
    def largestPalindrome(self, n: int, k: int) -> str:  
        if k == 1: return '9' * n  
        m = (n + 1) // 2 if n % 2 else n // 2  
        pow10_mod = [1] * n  
        for i in range(1, n):  
            pow10_mod[i] = (pow10_mod[i-1] * 10) % k  
        coeff = []  
        for i in range(m):  
            if n % 2 == 0 or i < m - 1:  
                c = (pow10_mod[n-1-i] + pow10_mod[i]) % k  
            else:  
                c = pow10_mod[n-1-i] % k  
            coeff.append(c)  
        # Backward DP: which remainders are reachable?  
        dp_backward = [set() for _ in range(m + 1)]  
        dp_backward[m].add(0)  
        for i in range(m-1, -1, -1):  
            current_coeff = coeff[i]  
            for d in range(10):  
                if i == 0 and d == 0: continue  
                contrib = d * current_coeff  
                for r in dp_backward[i+1]:  
                    dp_backward[i].add((r + contrib) % k)  
        # Greedy forward pass  
        first_half = []  
        current_remainder = 0  
        for i in range(m):  
            for d in range(9, -1, -1):  
                if i == 0 and d == 0: continue  
                contrib = d * coeff[i]  
                target = -(current_remainder + contrib) % k
```

```

        if target in dp_backward[i+1]:
            first_half.append(str(d))
            current_remainder = (current_remainder + contrib) % k
            break
    first_half_str = ''.join(first_half)
    if n % 2:
        return first_half_str + first_half_str[::-1][::-1]
    else:
        return first_half_str + first_half_str[::-1]
</code>
<stdin>3
5</stdin>
</tool>

```

#### Tool Response

```

completed.
<budget> Remaining turns: 3, Remaining tokens: 41605 </budget>

```

#### Assistant – Turn 4 (python-stress): Efficiency confirmed

```

<think>
... Now let's test the DP solution with large inputs to
confirm it runs within the time limit ...
</think>

<tool: python-stress>
test_cases = [(10**5, 9), (10**5, 2), (10**5, 5)]
for n, k in test_cases:
    start = time.time()
    result = Solution().largestPalindrome(n, k)
    elapsed = time.time() - start
    print(f"n={n}, k={k} Time: elapsed:.3fs PASS")
</tool>

```

#### Tool Response

```

completed. [stdout]n=100000, k=9 Time: 0.557s PASS
n=100000, k=2 Time: 0.158s PASS
n=100000, k=5 Time: 0.152s PASS[/stdout]
[performance] Execution Time: 0.959s, Peak Memory: 55.1 MB
<budget> Remaining turns: 2, Remaining tokens: 39572 </budget>

```

**Turns 5–6.** Tests small examples ( $n=1, k=4$ ;  $n=3, k=5$ ;  $n=5, k=6$ ) to verify correctness; all pass.

#### Assistant – Final Submission

```

<think>
Solution passes all tests and runs well within the time limit.
</think>

(submits the DP code from Turn 3; passes all hidden tests)

```

### J.2.3 Interpretation

Both models start with brute-force and both discover the timeout at  $n=10^5$ . The critical difference is what happens *after*: the low-coverage model has already exhausted its tool budget on minor variations and submits the brute-force code; the high-coverage model invests its remaining turns in developing a DP formulation that reduces complexity from  $O(n \cdot 10^m/k)$  to  $O(m \cdot k)$ .

### J.3 Discussion

These two trajectories make the frontier concrete:

- **hard/770 (Falling Bars):** Both models initially try efficient reverse-processing. The low-coverage model *pivots* to brute-force simulation when it fails; the high-coverage model stays committed to the efficient-but-wrong approach.
- **hard/680 (K-Palindrome):** Both models start with brute-force and discover it times out. The high-coverage model *pivots* to dynamic programming; the low-coverage model submits the slow code.

The pattern is symmetric: each model is more likely to *abandon a failing strategy* in the direction its training reward incentivizes. The low-coverage model, never penalized for timeouts during training, readily falls back to correct-but-slow algorithms, while the high-coverage model, trained against full stress tests, readily develops efficient algorithms even when correctness is uncertain. Neither behavior dominates across all problems—which is why interpolation and extrapolation can access solutions that no single endpoint produces.